January 2013

The Role Of Tumor-Associated Macrophages In Human Skin Cancer

Nika Cyrus
Yale School of Medicine, nikacyrus@gmail.com

The Role of Tumor-associated Macrophages in Human Skin Cancer

A Thesis Submitted to the
Yale University School of Medicine
in Partial Fulfillment of the Requirements for the
Degree of Doctor of Medicine

by

Nika Cyrus

2013

ABSTRACT

Inflammation has long been associated with tumorigenesis. Macrophages are cells of the innate immune system, whose density within tumors correlates with a worsening clinical prognosis in most types of tumors. Macrophages have been demonstrated to contribute to the initiation, growth, invasion, and metastasis of tumors. We hypothesized that macrophage density and phenotype differs between squamous cell carcinomas and basal cell carcinomas, two skin cancers with relatively aggressive and indolent clinical behaviors, respectively. Through immunohistochemical analysis, we determined that squamous cell carcinomas have a 5-fold higher density of macrophages than basal cell carcinomas. Tumor-associated macrophages exhibit two classic states of activation. M1 macrophages are inflammatory and are involved in clearance of microorganisms and tumor cells. By contrast, M2 macrophages are involved in tissue remodeling, angiogenesis, and are tumor-promoting. Using flow cytometric analysis of fresh clinical specimens, we determined that macrophages from squamous cell carcinomas express significantly higher levels of M1 (CD40, CD127) and M2 (arginase I) markers as well as higher levels of MMP-9, a pivotal enzyme in tumor matrix remodeling and tumor invasion, than macrophages from the basal cell carcinomas. To determine whether the Toll-like receptor (TLR) agonist imiquimod, an FDA-approved treatment for superficial basal cell carcinoma and actinic keratoses, alters the activation state of tumor-associated macrophages, we studied *in vitro* and *in vivo* effects of imiquimod on macrophages. We determined that imiquimod activates primary macrophages from human squamous cell carcinoma to an M1, pro-inflammatory immunophenotype. This phenotype was

associated with enhanced macrophage-induced apoptosis of cultured epidermoid carcinoma cells and enhanced phagocytosis of fluorescently labeled tumor cells. Our findings suggest that tumor-associated macrophages play a critical role in pathophysiology of two common human skin cancers. Further, we provide a novel mechanism of action of imiquimod, which provides potential insights in the utilization of immunomodulatory therapies in the treatments of a wider variety of cancers.

ACKNOWLEDGEMENTS

I would like to express my gratitude to the following individuals and departments at Yale University School of Medicine for their invaluable advice and contributions to my thesis research project through my thesis year:

Oscar Colegio MD PhD, My Thesis Mentor, Department of Dermatology

Allison Hanlon MD PhD, Department of Dermatology

Samuel Book MD, Department of Dermatology

Robert Tigelaar MD, Department of Dermatology

Stephanie Eisenbarth MD PhD, Department of Laboratory Medicine

Ruslan Medzhitov, HHMI, Department of Immunobiology

David Leffell MD, Department of Dermatology

Carolyn Brokowski, Department of Dermatology

Quynh Chu, Department of Dermatology

Thach Chu, Department of Dermatology

Howard Hughes Medical Institute

Yale University Department of Dermatology

Yale University, Section of Dermatologic Surgery and Cutaneous Oncology

Yale University Department of Immunobiology

TABLE OF CONTENTS

INTRODUCTION

Inflammation is recognized as being important for tumorigenesis and was recently proposed as the seventh hallmark of cancer (1-3). The inflammatory infiltrate in tumors most commonly consists predominantly of macrophages, T cells, neutrophils, natural killer (NK) cells – but includes other hematopoietic cells (4). Among these cells, macrophages are the most numerous cells in this tumor infiltrate (5). Tumor-associated macrophages (TAMs) are closely involved in multiple stages of carcinogenesis: they contribute to initiation, growth, invasion, and metastasis of tumors through production of a diverse array of cytokines, growth factors, pro-angiogenic factors, and matrix metalloproteinases (6-8).

The most common cancer in the United States is non-melanoma skin cancer with an estimated 1.3 million cases each year (9). The incidence of NMSC is increasing worldwide (10-12). It is essential to understand macrophage phenotypic characteristics in tumors of diverse clinical behavior to understand which factors correlate with tumor growth, invasion and metastasis. The two most common forms of NMSC are basal cell carcinoma (BCC) and squamous cell carcinoma (SCC) (13). BCC and SCC are ideal tumors to consider in study of TAMs in humans as they represent two common epidermal neoplasms that behave differently clinically. BCCs only grow and invade locally and do not metastasize (14, 15). In contrast, SCCs are more invasive and can metastasize in late stages (9). Sun exposure, specifically UV-B radiation, is considered to be one of the most important environmental factors involved in initiation of SCC (9). UV-B exposure directly leads to DNA and RNA damage through formation of pyrimidine dimers (13). A limited number of studies have examined the role of macrophages in skin cancer. In

BCC, it has been shown recently that the number of TAMs infiltrating the tumor directly correlates with depth of tumor invasion and microvessel density (18). In cutaneous SCC, TAMs are shown to be a major source of VEGF-C, a critical lymphangiogenic factor (19). Therefore, study of *in vivo* TAMs in SCC and BCC represents a suitable strategy for further understanding of cutaneous carcinogenesis.

TAMs classically exhibit two states of activation known as M1 and M2 states. Macrophages are polarized in response to Th1 cytokines, LPS and IFN-gamma, into an M1 state (2, 20, 21). On the other hand, in response to Th2 cytokines, IL-4 and IL-13, macrophages enter an M2 state (2, 21). M1 macrophages are inflammatory and produce a variety of pro-inflammatory factors such as IL-1β, TNF-α, and IL-6 (2, 21). In general, M1 macrophages are involved in clearance of microorganisms. M2 macrophages on the other hand are involved in type 2 inflammation, tissue remodeling, angiogenesis, and are believed to promote tumor growth (2, 22, 23). M2 macrophages produce high levels of Interleukin-10 (IL-10) and arginase I and express numerous scavenger receptors (2). The classical M1-M2 paradigm has been recently revealed to represent two ends of a spectrum that can also include heterogeneous states of activation. It has been shown in multiple studies that macrophages can show mixed states of activation and there are multiple sub-populations of TAMs (24, 25).

Imiquimod is a topically used imidazoquinoline drug approved by the Food and Drug Administration (FDA) for treatment of superficial BCCs, Actinic Keratoses, and warts (13). It is known to possess antiviral and anti-tumoral effects. Mechanistically, imiquimod is an immune response modifier and can also lead to direct tumor cell death, possibly by down-regulation of BCL-2 anti-apoptosis gene (26). Imiquimod has been

shown to be a specific agonist of TLR-7 in macrophages, a major arm of the innate immune system. Imiquimod and resiquimod (R848) activation of macrophages is MyD88-dependent (27, 28). We sought to characterize how TAMs are modulated by imiquimod both *in vivo* and *in vitro*. We utilized both imiquimod and resiquimod in our experiments. We hypothesized that imiquimod will act as a modulator of TAM phenotype towards a tumoricidal state and away from trophic, tumor-promoting functions.

STATEMENT OF PURPOSE & HYPOTHESIS

The specific aims and hypotheses of this thesis project are as follows:

1) **Compare density of TAMs in human SCCs and BCCs**:

   Hypothesis: Given that increasing macrophage density typically correlates with tumor aggressiveness, we hypothesize that there will be a higher density of TAMs in SCCs as compared to BCCs.

2) **Characterize *in vivo* M1-M2 immunophenotype of TAMs in SCC and BCC tumors using flow cytometry and determine whether tumor-derived soluble factor(s) are sufficient to reproduce this phenotype in *vitro***:

   Hypothesis: TAMs have differential activation in SCCs and BCCs, which may contribute to their distinct clinical behavior. Soluble factors derived from these tumors can induce human macrophages to assume an immunophenotype similar to the *in vivo* immunophenotype of TAMs in SCCs and BCCs.

3) **Determine whether imiquimod can modulate TAM immunophenotype *in vivo* and *in vitro*.**

   Hypothesis: Imiquimod can polarize macrophages towards an M1, pro-inflammatory state.

4) **Determine whether imiquimod-primed macrophages can induce apoptosis of tumor cells and enhance phagocytic capacity of macrophages for tumor cells**

   Hypothesis: Imiquimod can activate macrophages to induce apoptosis of carcinoma cells. Furthermore, imiquimod can enhance phagocytosis of carcinoma cells by macrophages.

METHODS

All subjects participated voluntarily in this study after signing an informed consent. Human Investigation Committee approval was obtained prior to start of research project. Subjects were not exposed to any risks in this study as they were undergoing routine cutaneous surgery for the excision of skin cancer and agreed to donate the specimen for research. All experiments detailed in the subsequent sections were carried out by the author in Yale Departments of Dermatology and Immunobiology except for immunohistochemical staining of the SCC and BCC samples, which was performed by the Yale Dermatopathology Lab. Tumor histology was evaluated by board-certified dermatopathologists to ensure that tumors were either SCC or BCC prior to being included in experiments.

I) Immunohistochemistry:

Biopsy-proven BCCs (n=6) and SCCs (n=5) were confirmed by a dermatopathologist and utilized for immunohistochemical staining of TAMs. Tissue sections were stained with hematoxylin and eosin and CD68 antibody by the Yale Dermatopathology Lab. CD68+ macrophages were visualized at 40X magnification with OTIPHON Nikon microscope. Numbers of TAMs per 40X HPF were counted with ImageJ by two independent researchers.

II) Mechanical and enzymatic digestion of cutaneous tumors into single cell suspensions:

Biopsy-proven cutaneous SCC and BCC extirpated by Mohs micrographic surgery were used after obtaining informed consent. The debulked tumor specimens were transported on ice. The tumors were weighed, and the length and width were measured to nearest millimeter. Next, the tumor was minced using surgical scissors into small pieces, all less than 2 mm in length. The digestion buffer consisting of Liberase TM at final concentration of 26 Wünsch/mL and DNase in PBS with calcium and magnesium was prepared. The specimen was then transferred to 10-20 mL of digestion buffer depending on tumor weight in a 50 mL conical tube. The digestion was carried out in a shaking incubator at 37 ºC for 90 minutes. After the end of the incubation period, 0.1 M Ethylenediaminetetraacetic acid (EDTA) was added at dilution of 1:50 and the digest was placed on ice for 5 minutes to stop the enzymatic reaction. In order to acquire a single cell suspension, the tumor digest was passed through a custom metal sieve designed to remove larger clumps of undigested matter. Next, the filtered liquid was passed through a 70 µm cell strainer. This resulted in a homogenous cell suspension that was subsequently centrifuged at 1300 rpm for 5 min at 4 ºC. After centrifugation, the pellet was re-suspended in ACK lysis buffer to lyse erythrocytes. The reaction was stopped with FACS buffer (0.5 % fetal bovine serum in PBS), and after centrifugation the final purified cell suspension was suspended in FACS buffer. Using trypan blue staining cell viability was assessed and cell count was approximated.

III) Immunophenotyping of Macrophages in human SCCs and BCCs

The final tumor digests were plated in a 96-well plate at 1-2 million cells / well consisting of an unstained condition, and three separate panels designed to determine M1 and M2 activation states in tumor associated macrophages. Prior to staining macrophages, Fc-block was carried out by adding 50 µL of 1:200 diluted human Fc-Block solution (eBioscience) and the sample was incubated for 20 minutes on ice, in the dark. The sample was then washed with FACS buffer. The samples were then stained by adding 50 uL of surface antibodies CD127-PerCP-Cy5.5, CD40-PerCP-Cy5.5, CD45-APC, and CD163-APC at recommended dilutions (eBioscience, Biolegend). The samples were incubated for 15 minutes in dark on ice. 150 uL of FACS buffer was added to each sample, followed by centrifugation at 1300 rpm for 5 minutes, and removal of supernatant. The wash was repeated a second time.

Utilizing the standard protocol for intracellular staining from BD Biosciences, the samples were processed. The intracellular stains CD68-PE (2.5 uL per million cells), arginase I-CFS (10 µL per million cells, R&D systems) and MMP-9 CFS (10 µL per million cells, R&D Systems) were added to each sample in a final volume of 50 µL per well. The intracellular staining was carried out per manufacturer's instructions (BD biosciences). All FACS analysis was carried out either immediately or within 12 hours with sample stored in dark and at 4 ºC. Single color controls were prepared utilizing BD Compensation beads (positive and negative beads) and the same antibodies used at identical dilutions per manufacturer's instructions. All antibodies had Fc-gamma chains that are appropriate for use with the Comp Beads. FACS analysis was carried out on BD FACS Calibur. The PMT voltages were adjusted using the unstained sample containing the purified tumor cell suspension processed identically as the stained samples while

replacing the staining steps with buffers. After setting appropriate voltages and gating on live cells based on Forward Scatter (FSC) and Side Scatter (SSC), the compensation was carried out with Comp Beads. Next, samples were analyzed with the BD FACS Calibur flow cytometer. To achieve statistical significance, 100,000-1 million events were collected for each sample. The acquired data was analyzed using FlowJo. The preparation techniques, staining procedures, and antibody dilutions, and data analyses were identical for both BCCs and SCCs allowing direct comparison of FACS data.

IV) Stimulation of THP-1 cells (human monocytic cell line) with tumor-conditioned media

Tumor-conditioned media was prepared by manual mincing of SCC and BCC specimens with surgical scissors and re-suspending in complete RPMI media. The tumor-media suspension was incubated at 37 ºC in a humidified tissue culture (TC) incubator. The tumor supernatant was then carefully aspirated, centrifuged, and sterile filtered with 0.45 µm syringe filter. The tumor-conditioned media were stored at -80°C for future experiments. For in vitro, stimulation of THP-1 cells (human monocytic cell line), 1 million THP-1 cells were plated in 1 mL of tumor-conditioned media in sterile six-well tissue culture plates and incubated for 48 hours. The THP-1 cells were then utilized for flow cytometric immunophenotyping as previously described.

V) Co-culture of human SCC, peri-tumoral skin with THP-1 cells

For co-culture assay, fresh Mohs debulked SCC specimens and peri-tumoral normal skin from the same patient were manually dissociated with surgical scissors and placed in

complete media in the Transwell cell culture insert (1 µm) immediately after surgery. 1 million THP-1 cells were plated in 1 mL of complete RPMI in six-well plates. The co-culture assay was carried out for 48 hours and 72 hours in 37°C humidified TC incubator. A negative control with no co-culture was also included. At the end of incubation time, the upper insert was removed, and THP-1 cells were washed and utilized for flow cytometric immunophenotyping as described previously.

VI) *In vitro* study of imiquimod's effect on THP-1 cells

THP-1 cells were plated in RMPI complete at density of 1 million/mL in sterile six-well or twelve-well tissue culture plates. The control conditions included negative control (plain RPMI complete), positive control (LPS 100 ng/mL, human IFN-gamma 20 ng/mL in RPMI complete. For *in vitro* study of mechanism of imiquimod, THP-1 cells were incubated in multi-well plates as follows: 1) Negative control. 2) Positive control 3) 50 µg/mL imiquimod (Invivogen) 4) 10 µg/mL resiquimod (Invivogen). THP-1 cells were incubated for 48 hours in 37°C humidified TC incubator (5 % CO_2). After 48 hours, cells were harvested with cold PBS and processed for flow cytometry. Briefly, cells were Fc-blocked and stained with CD40, CD127, arginase I, MMP-9, CD45, and CD68 as described previously, and analyzed with BD FACS Calibur. Data was analyzed with FlowJo: Live cells were gated upon based on FSC and SSC. CD68+CD45+ THP-1 cells were next selected and histograms created for all the markers mentioned. For investigation of imiquimod's effects on TAMs, THP-1 cells were plated in sterile 12-well tissue culture plates with the following conditions included: BCC-conditioned media with and without 50 µg/mL imiquimod, SCC-conditioned media with and without imiquimod

50 µg/mL, and RPMI complete serving as negative control. After 48 hours of incubation in humidified 37°C TC incubator, THP-1 cells were harvested, washed, and prepared for FACS immunophenotype of M1, M2 and MMP-9 as previously described.

VII) *In vivo* immunophenotype of TAMs imiquimod-treated patient

For *in vivo* experiments, we obtained a fresh SCC debulk specimen in a patient treated with 2.5 % imiquimod for two weeks prior to surgery. A comparable SCC in a patient not treated with imiquimod was analyzed on the same day. We used the optimized enzymatic dissociation protocol, previously described, to create single cell suspensions. Next, the cell suspension was prepared for FACS immunophenotype and processed for both imiquimod treated SCC and control SCC.

VIII) Apoptosis assay for evaluation of imiquimod-primed macrophages effect on A431 carcinoma cells

THP-1 cells were stimulated with 50 µg/mL imiquimod in RPMI complete media. THP-1 cells in RPMI complete media were used as negative controls. THP-1 cells were incubated for 48 hours in humidified TC incubator at 37°C. At the end of incubation, the THP-1 cells' suspension was centrifuged at 1300 RPM for 5 min, and the supernatant was aspirated. Next, the pellet was re-suspended in 20 mL of cold PBS. The suspension was re-centrifuged and all of the supernatant was carefully aspirated. The final THP-1 cell pellet was re-suspended in DMEM complete and placed on ice. A431 epidermoid carcinoma cells were plated in sterile non-tissue culture six-well plate at density of 1 million per well in EMEM complete. Transwell cell culture insert (1 µm) were placed on

top of each well using sterile forceps. 1 million THP-1 cells from control and imiquimod pre-treated group were added to Transwell cell culture inserts in the six-well plate. The THP1-A431 co-culture plate was then incubated in a humidified TC incubator at 37 ºC for 72 hours. At the end of incubation, the upper cell culture insert containing THP-1 cells was carefully removed. A431 epidermoid carcinoma cells were gently trypsinized off the wells and re-suspended in EMEM complete. Annexin V FITC apoptosis kit from eBioscience was used for the measurement of rate of apoptosis per manufacturer's instructions. The tumor cells were first washed with cold PBS and then binding buffer. The samples were re-suspended in 200 µL of binding buffer. Five µL of Annexin V FITC was added to each well and mixed. The samples were then incubated for 10 minutes in dark. After completion of staining, the samples were washed with 200 µL of binding buffer. The samples were re-suspended in 200 µL of binding buffer and 5 µL of propidium iodide staining solution (eBioscience) was added. The samples were analyzed using FACS BD Calibur and compensations were carried out using unstained and BD compensation beads. Annexin V staining was calculated using the FITC channel and propidium iodide was measured in PerCP channel. Data was analyzed using FlowJo and Prism. Rate of early apoptosis was calculated as percentage of FITC positive cells. Rate of late apoptosis was calculated as percentage of FITC/PerCP double positive cells, which stained for both Annexin V-FITC and propidium iodide.

IX) Phagocytosis assay for investigation of phagocytic capacity of imiquimod-primed macrophages

THP-1 cells were stimulated using imiquimod 50 µg/mL in RPMI complete and control RPMI complete as previously described for 48 hours in humidified 37 ºC TC incubator. After end of incubation, the samples were centrifuged and the supernatants were aspirated. Twenty mL of cold PBS was used to wash the THP-1 cells. After centrifugation, all of the supernatant was carefully aspirated. The THP-1 cells were kept on ice. A431 epidermoid carcinoma cells were then labeled with PE fluorescent dye using PKH26 Red Fluorescent Cell Linker per manufacturer's instructions (Sigma Aldrich). Briefly, A431 cells were first washed with serum-free media, and then re-suspended in 1 mL of Diluent C. PKH26 dye solution was prepared in 1 mL of Diluent C by adding 4 uL of PKH26 dye. The prepared dye solution was rapidly added to the cell suspension and mixed thoroughly through pipetting up and down. The sample was then incubated for 2 minutes and serum was added to stop the reaction. The sample was then centrifuged at 400g for 10 minutes. The supernatant was aspirated and cells were suspended in 10 mL of complete media and transferred to a new tube. The cells were washed an additional two times with complete media prior to being used in experiments.

PE-labeled tumor cells were then used for the purpose of phagocytosis experiments. One million THP-1 control cells were mixed with 6 million PE-labeled epidermoid carcinoma cells in a 50 mL conical tube, which served as the control group. One million THP-1 cells pre-treated with imiquimod were mixed with 6 million PE-labeled epidermoid carcinoma cells, serving as the imiquimod group. Another condition included only THP-1 control cells without PE-labeled tumor cells to serve as cell-free control. The samples were then incubated in a shaking TC incubator for 60 minutes at 200 rotations per minute (RPM). After incubation, the samples were prepared for flow

cytometry as previously described using CD45-APC stain. Briefly, the samples were re-suspended in FACS buffer and were Fc-Blocked using human Fc Block (eBioscience). Next, the samples were washed once with FACS buffer. CD45 APC was utilized to stain the samples (5 uL per 1 million cells) for 15 minutes in dark on ice. Next, the samples were washed with 200 uL of FACS buffer two times. The samples were analyzed on FACS Calibur. Rate of phagocytosis was determined by first gating on THP-1 cells using CD45-APC. After gating on macrophages, the percentage of PE-positive macrophages was used as marker of phagocytosis.

X) Statistical analysis

FACS data were analyzed with FlowJo. All statistical tests were performed with Prism utilizing unpaired, two-tailed Student's t test.

RESULTS

The characteristics of subjects in this study for Immunophenotyping of TAMs in NMSCs, *in vitro* experiments, and imiquimod mechanistic experiments are shown in Table A. Age, gender, diagnosis, duration of lesion, and history of recurrent skin cancer for each patient are listed. Histopathologic diagnosis and features, tumor dimensions (mm), and anatomic locations are also shown (Table A).

Human cutaneous SCCs have significantly higher density of TAMs compared to BCCs.

In order to determine the density of TAMs in human cutaneous SCC, we stained H&E slides of biopsy-proven SCCs and BCCs with CD68 and quantified number of TAMs per high-power field (HPF). Analysis of SCCs (n=5) and BCCs (n=6) revealed that there is significantly higher density of TAMs in SCC compared to BCC (Figure 1b, p value < 0.0001, unpaired two-tailed student t test). Representative histology of SCC and BCC are shown in Figure 1a demonstrating the distinctly different density of CD68+ TAMs in these two common forms of NMSC.

Development of a method to analyze TAMs from primary SCC and BCC tumors

Utilizing a combination of manual mechanical dissociation and enzymatic digestion with Liberase (Roche), we obtained a viable suspension from human SCCs and BCCs from multiple patients. All preparation was performed on the day of the Mohs micrographic surgery on patients with biopsy-proven cutaneous carcinomas. To our knowledge this represents the first successful FACS analysis of tumor associated macrophages in human

cutaneous SCCs and BCCs. After optimization of the digestion process, we were able to obtain 5-30 million total cells from each tumor depending on weight. After the digestion process, cells were counted and trypan blue staining demonstrated that the cellular digest consisted of viable cells. The human tumor digest was then prepared for flow cytometric analysis of macrophages with multiple M1, M2, and TAM markers immediately after digestion. All FACS staining was performed on freshly digested specimens. Our immunophenotype panels were designed to characterize TAMs for their M1 and M2 polarization states. CD127 (IL-7 receptor) and CD40 (co-stimulatory receptor) were used as M1 markers (2, 24, 29, 30). Arginase I (2, 24) was used as an M2 marker. The advantage of FACS in comparison with immunohistochemistry is that multiple markers can be studied simultaneously and in a way to recognize multiple sub-populations. Given the recently recognized heterogeneity of TAM expression profile, FACS is an ideal method to detect distinct sub-populations of TAMs and also detect simultaneous M1 and M2 activation.

By FACS analysis, we gated on a clear CD68+ CD45+ TAM population from both SCCs and BCCs. CD45 was utilized in addition to the classic macrophage maker (CD68) to ensure that only leukocytes were included in the analysis and tumor cells are excluded. First, we selected for live cells by gating on FSC and SSC. The plot of CD68-PE *versus* CD45-APC demonstrates a clear double positive population that represents TAMs in human BCC and SCC (Figure 2a). In addition to CD68, we also used CD163, as another marker of TAMs in the skin. Percentage of C68+CD45+ TAMs in the tumor digest was not significantly different between SCCs and BCCs (mean 2.7 % in SCC *versus* 2.2 % in BCC. $p > 0.05$). This is in contrast to the findings from quantitative

immunohistochemistry and may represent a limitation of isolating individual living cells from tissue.

TAMs from SCCs and BCCs have different degrees of polarization.

Based on our analysis of published microarrays of NMSC, human cutaneous SCCs and BCCs have distinct microarray gene profiles of CD68, MMP-9 and arginase I (Figure 3). We analyzed published whole tumor microarrays of human SCCs (n=13) and BCCs (n=11) and Normal skin (n=4) to investigate expression profiles of CD68, arginase I, MMP-9 (31). Mean values of microarray signals for MMP-9, CD68, arginase I and SEM were calculated. Percentage present (%) was defined as percentage of all samples with significant p-values indicating that the gene is present in microarray profile of the tumor. In these expression arrays, CD68 was more highly expressed in SCC compared to BCC, and both skin cancers had higher CD68 expression than normal skin (Figure 3). MMP-9 shows stronger expression in SCC as compared to BCC and normal skin (Figure 3). In addition, arginase I (probe 1) was present in significantly higher percentage of SCC tumors as compared to BCC (Figure 3). In a similar fashion, arginase I (probe 2) was present in 36% of SCC tumors yet completely absent from BCC and normal skin (Figure 3). The results of whole tumor microarray analysis showed that CD68 (macrophage marker), arginase I (M2), and MMP-9 (TAM marker) had higher expression levels in SCC as compared to BCC and normal skin control. The results of this whole tumor microarray analysis suggested differential activation of TAMs in SCC *versus* BCC.

To address this question using FACS analysis, SCCs (n=7) and BCCs (n=7) were processed for flow cytometric immunophenotyping of TAMs using an optimized method

of enzymatic dissociation (Figure 2). We compared levels of arginase I and MMP-9 in TAMs in SCC (CD68+CD45+) in comparison with other leukocytes (CD68-CD45+) (Figure 2a-b). We observed significantly higher levels of both arginase I and MMP9 in TAMs as compared to other WBCs (Figure 2b). In addition, TAMs had higher levels of both arginase I and MMP-9 as compared to tumor cells (CD68-CD45-, data not displayed).

Immunophentyping of TAMs in human NMSCs demonstrated that TAMs in cutaneous SCC had significantly higher levels of MMP-9 compared to cutaneous BCC. This was demonstrated by a reproducible shift in histograms of MMP9-CFS observed in BCC and SCC (Figure 2c). In addition, intracellular human arginase I intracellular staining revealed that TAMs in SCC expressed higher levels of arginase I compared to TAMs in BCC (Figure 2c). This demonstrated that macrophages in SCC are M2 activated whereas macrophages in BCC have minimal M2 activation. In terms of expression of M1 markers CD127 and CD40, macrophages showed higher levels of both markers in as compared to BCC (Figure 2c-d). This trend was reproducible in multiple tumors from different patients as shown by overlaid representative histograms of CD40-PerCP and CD127-PerCP in SCC (red) and BCC (blue) (Figure 2c-d). Similar results was seen in CD68+CD163+ as shown by significant shifts in histograms of arginase I (M2), MMP9 (TAM), CD40 (M1), and CD127 (M1) (Figure 2d).

Sub-population analysis of SCC and BCC TAMs demonstrates the varied nature of the TAM polarization state

The multi-color nature of flow cytometry allowed us to utilize the data for sub-population analysis. In order to enhance analysis of data, M1 *versus* M2 graphs were created to help us delineate M1 and M2 activation of TAMs in SCC *versus* BCC. CD127 *versus* arginase I graphs demonstrated the following reproducible pattern as shown in tumors from different patients: TAMs from SCC are both M1 (CD127) and M2 (arginase I) activated. By comparison, TAMs from BCC mainly show a state of quiescence and demonstrate lower M1 and M2 activation (Figure 4). In BCC, a quadrant plot was used to analyze distribution of macrophage polarization. Macrophages are in a baseline state, meaning neither M1 nor M2 activated (78.7 %), only M1 activated (7.07 %), only M2 activated (5.82 %), or express both M1 and M2 markers simultaneously (8.37 %) (Figure 4). In order to compare this polarization pattern, we carried out a similar analysis in two SCCs. In a smaller-sized SCC, there are four distinct populations that can be appreciated in the FACS plot: baseline state (7.85 %), M1 only (42.8 %), M2 only (5.49 %), both M1 and M2 activation (23.6 %). In a larger SCC, we delineated two populations: the majority of macrophages are M1 and M2 activated (94.1 %) and the rest are in a baseline state (4.02 %). This type of sub-population analysis demonstrates that TAMs are not in one particular polarization program but rather can express M1 and M2 markers either individually or simultaneously (Figure 4).

TAMs in SCCs are M1 & M2-activated in comparison with peri-tumoral normal skin-resident macrophages

Immunophenotype of tumor-associated macrophages in cutaneous SCC was determined using flow cytometry and compared directly to tissue resident macrophages in peri-tumoral normal skin from the same subject. Biopsy-confirmed SCCs (n=3) from Mohs debulked tumor specimens and peri-tumoral normal skin (n=3) from the same patient were obtained. Both specimens were digested enzymatically and processed in an identical fashion for flow cytometric immunophenotype as previously described. The experiment was performed a total of three times together with corresponding peri-tumoral normal skin. The results of this experiment show that TAMs in human SCCs are M1 polarized as demonstrated by an increase in CD127 and CD40 levels as compared to peri-tumoral normal skin (Figure 5). In addition, TAMs are also M2 polarized (increased arginase I) and produce increased levels of MMP-9 as compared to tissue resident macrophages in normal skin (Figure 5).

Co-culture of human SCCs with naive THP-1 macrophages reproduces TAM polarization *in vitro*

We designed an *in vitro* co-culture assay with human SCC and THP-1 cells to investigate whether a *paracrine*, non-contact-dependent communication between TAMs and SCC cells can account for our *in vivo* observation of heterogeneous M1 and M2 polarization. Biopsy-confirmed cutaneous SCC from Mohs debulked tumors was mechanically dissociated with sterile surgical scissors and suspended in RPMI with 10 % FCS in a 1 um Transwell cell culture insert. In the lower chamber, THP-1 macrophages were plated at 1 million cells/mL. After 48 hours and 72 hours of co-culture, the upper insert was removed and THP-1 macrophages were analyzed by FACS for M1, M2, and

MMP-9 expression. For a control, we used peri-tumoral normal skin from the same patient, which was surgically removed from an adjacent anatomical location at the same time and co-cultured the dissociated skin with THP-1 macrophages. As a second negative control, THP-1 macrophages were grown fresh RPMI, without any other cells plated in co-culture. To analyze the state of polarization by FACS, we first gated live cells, followed by gating CD68+CD45+ cells, which represented the majority of THP-1 macrophages. THP-1s were polarized to heterogeneous M1 and M2 activation through paracrine interaction with human SCC tumor suspension (Figure 6). THP-1s displayed characteristics of M1 and M2 activation as demonstrated by significant shifts in arginase I, CD127 and CD40 compared to peri-tumoral normal skin and non-stimulated THP-1, which closely correlates with our *in vivo* findings of immunophenotype of TAMs in human SCCs. In addition, MMP-9 production is significantly increased through paracrine signaling of SCC cells co-cultured with THP-1s as compared to peri-tumoral normal skin co-culture (Figure 6). Similar results are observed after 48 hours and 72 hours of incubation with SCCs from different patients.

Soluble factor(s) in tumor-conditioned media from SCC and BCC differentially polarize human macrophages to a TAM phenotype

Conditioned media was prepared from dissociated SCCs (n=3) and BCCs (n=3) *in vitro*. Biopsy-confirmed Mohs debulked tumor specimens were dissociated in a sterile environment and placed in RPMI-complete for 24 hours. The tumor supernatant was carefully aspirated and sterile filtered. THP-1 cells were incubated in the presence of control RPMI media, SCC-conditioned media, and BCC-conditioned media for 48 hours

in a humidified TC incubator at 37 ºC. Human macrophages demonstrate differential activation as a result of incubation in SCC- and BCC-conditioned media (Figure 7). THP-1 cells incubated in SCC-conditioned media showed significant M1 and M2 polarization compared to either BCC or THP-1 cells control as demonstrated by significant shifts in histograms of CD40 (M1), CD127 (M1), and arginase I (M2) (Figure 7). In addition, MMP-9 production by THP-1 cells was strongly induced by SCC-conditioned compared to BCC-conditioned media (Figure 7). The results conform to findings from co-culture of THP-1 cells and SCC, and *in vivo* phenotype of TAMs in SCCs *versus* BCCs. Soluble factor(s) present in tumor-conditioned media are sufficient to polarize THP-1 cells *in vitro* towards the respective TAM phenotype we observed *in vivo* in SCCs and BCCs.

Imiquimod induces M1 activation of THP-1 cells *in vitro* as demonstrated by flow cytometry

To determine, whether TLR-7/8-agonists were sufficient to polarize our THP-1 monocytic cell line to an M1 state, we carried out *in vitro* experiments with both imiquimod and resiquimod, an investigational analogue of imiquimod. THP-1 cells were plated in the control media or in media containing 50 µg/mL imiquimod or 10 µg/mL resiquimod. Positive controls of the TLR-4 agonist LPS (100 ng/mL) and IFN-gamma (20 ng/mL) were included. After 48 hours, THP-1 cells were analyzed by flow cytometry for expression of M1 markers (CD40 and CD127). In analysis of results, live cells were gated on based on FSC and SSC. CD68+CD45+ cells were then selected and histograms of M1 markers were produced. Interestingly, imiquimod induced significant M1 polarization as shown by histogram shifts in CD40 and CD127 fluorescent intensity of

macrophages compared to negative control (Figure 8). The positive control with LPS and IFN-gamma induced the expected shift in M1 markers (Figure 8). Resiquimod (TLR-7/8 agonist) also induced M1 markers (Figure 8). Together, the results of these series of experiments demonstrate a possible immunologic mechanism for imiquimod, which involves amplification of M1 polarization state of macrophages.

Imiquimod treatment leads to M1 polarization of TAMs in SCC *in vivo*

We obtained a fresh SCC specimen from a patient treated for 2 weeks with topical 2.5 % imiquimod treatment to scalp tumor. A comparable SCC was utilized as control. Both tumors were processed in parallel for flow cytometric analysis. *In vivo* immunophenotype of CD68+CD45+ macrophages was determined with FACS. In agreement with *in vitro* experiments, imiquimod treatment polarized TAMs to an M1 activation state (Figure 9). We observed significant induction of CD40 by imiquimod as shown in Figure 9, with a majority of macrophages M1 polarized (94.5 %) in contrast to control SCC TAMs that were 45.8 % M1 polarized. Coordinately, there was also a positive shift in another M1 marker, CD127 (Figure 9). Interestingly, imiquimod treatment leads to down-regulation of the tumor promoting metalloproteinase, MMP-9 by TAMs (Figure 9). Arginase I levels did not show an observable shift in this case (Figure 9). In summary, imiquimod treatment leads to M1 activation of TAMs and down-regulation of MMP-9.

Imiquimod is a dual immunomodulator of TAMs *in vitro* through M1 activation and M2 inhibition

We attempted to investigate whether imiquimod plays an immunomodulatory role for TAMs in the tumor microenvironment. To answer this question, we devised an experiment that models the tumor microenvironment. Briefly, THP-1 cells were plated in tumor-conditioned media from either SCC or BCC. The conditioned media was prepared from fresh Mohs debulked tumor specimens that were mechanically dissociated and placed in RPMI-complete for 24 hours, followed by sterile filtration with 0.45 μm filter and freezing at -80 ºC. THP-1 cells were plated in either BCC- or SCC-conditioned media in the presence or absence of 50 μg/mL imiquimod. After 48 hours of incubation, THP-1 cells were analyzed by flow cytometry for M1 (CD127), M2 (arginase I) and MMP-9. THP-1 cells stimulated by SCC supernatant alone were M1 and M2 activated as seen by upregulation of MMP-9, arginase I, CD127, and CD40. Stimulation by BCC supernatant alone also causes M1 and M2 activation though to a lesser degree. The levels of M1 and M2 markers, in contrast, are significantly modulated by presence of imiquimod in tumor supernatants. The results of this experiment indicate that imiquimod plays an immunomodulatory role by up-regulating M1 polarization, while simultaneously down-regulating arginase I (M2) and MMP-9 production as seen in THP-1s exposed to BCC supernatant with imiquimod as compared to BCC supernatant without imiquimod (Figure 10). The arrows on the histograms indicate the direction of skewing induced by imiquimod (Figure 10). A similar pattern is observed in another experiment with THP-1 cells incubated in SCC-conditioned media in presence and absence of imiquimod (Figure 10). In conclusion, imiquimod lead to significant M1 activation and down-regulation of M2 polarization and MMP-9 production in macrophages primed in tumor-conditioned media (Figure 10).

Imiquimod-treated THP-1 cells induce apoptosis in human epidermoid carcinoma cells

In order to determine whether imiquimod can activate anti-tumoral capacity of macrophages, we designed an experiment using THP-1 cells and A431 epidermoid carcinoma cells. THP-1 cells were first primed by imiquimod or control media for 48 hours and then cells were washed. The resulting control and imiquimod-primed THP-1 cells were then utilized in a co-culture system with epidermoid carcinoma cells. The tumor cells were plated and control and imiquimod pre-treated THP-1 cells were placed in the upper Transwell insert. After 72 hours of incubation, we measured level of apoptosis in epidermoid carcinoma cells using Annexin FITC kit (eBioscience) and propidium iodide. This experimental setup is a non-contact-dependent system that allows exchange of soluble factors from THP-1 cells to tumor cells.

The level of apoptosis in tumor cells exposed to control THP-1 cells and imiquimod-primed THP-1 cells is shown in Figure 11. The graph shows propidium iodide-PerCP *versus* Annexin V- FITC staining (Figure 11). Early apoptosis was measured by determining the percentage of Annexin V-positive cells, which are negative for propidium iodide. The rate of early apoptosis was 12.2 % in the imiquimod group as compared to 8.47 % in control group (Figure 11). This demonstrates that imiquimod priming the THP-1 cells resulted in a higher level of early apoptosis of epidermoid carcinoma cells compared to naive THP-1 cells. Late apoptosis was measured as percentage of double positive cells for Annexin V-FITC and propidium Iodide-PerCP (Figure 11). Interestingly, level of late apoptosis was 6.16 % in the tumors cells co-

cultured with imiquimod primed macrophages as compared to 1.04 % in the tumor cells co-cultured with naive macrophages (Figure 11). These findings reveal a six-fold increase in the level of late apoptosis of tumor cells in the imiquimod-primed group as compared to the control group.

THP-1 cells primed with imiquimod phagocytose significantly more tumor cells compared to naive THP-1 cells

To whether imiquimod induces macrophage phagocytosis of tumor cells, we devised a phagocytosis assay using PE-labeled tumor cells and human macrophages primed with imiquimod. First, THP-1 cells were incubated in media with and without imiquimod for 48 hours. The THP-1 cells were then washed and used for tumor cell phagocytosis experiments. A431 epidermoid carcinoma cells were labeled with PE dye using PKH26 kit (Sigma Aldrich). The cell membrane PE labeling allows the phagocytized cells to be quantified using flow cytometry. PE-labeled epidermoid carcinoma cell were mixed with control or imiquimod-primed THP-1 cells in a ratio of 6:1 to mimic the *in vivo* tumor microenvironment. The samples were then incubated in a shaking TC incubator for 1 hour at 200 rpm. Samples were then prepared for flow cytometric analysis using CD45 APC.

The level of phagocytosis was determined by measuring the percentage of PE-positive, CD45+ macrophages (Figure 12). Interestingly, the rate of phagocytosis was 68.2 % in the imiquimod-primed macrophages as compared to 8.22 % in the control naive macrophages (Figure 12). The cell-free negative control had a background level of 0.27 % positive staining as expected (Figure 12). These findings demonstrate that imiquimod induces macrophages to phagocytose epidermoid carcinoma cells.

DISCUSSION

TAMs in cutaneous SCCs have higher levels of both M1 and M2 polarization than those TAMs in BCCs

We hypothesized that TAMs from SCC had a different level of activation than those from BCCs given their markedly different clinical features. To test this, we isolated tumor associated macrophages from SCCs and BCCs *in vivo* and characterized them with multiple panels utilizing florescent active cell sorting (FACS). FACS experiments on cutaneous neoplasms have been historically challenging due to technical difficulty of digestion of such highly collagenous tumors while preserving cell viability. This study presents a technical advance in the field by providing a simple, reproducible technique for creating a viable cell suspension of SCCs and BCCs that is suitable for flow cytometric analysis of the wide variety of cell types that make up these skin tumors. The FACS immunophenotype panel of TAMs in cutaneous SCCs demonstrates that macrophages have a heterogeneous activation state characterized by both M1 and M2 activation (Figure 2). Based on our flow cytometric immunophenotypes from multiple tumors (n=14), all from different patients, TAMs are consistently activated with profiles unique to SCCs *versus* BCCs, with SCCs demonstrating higher M1 and M2 activation (Figure 2). Our findings are in agreement with recent findings of M1 and M2 gene expression profile of TAMs in SCC (24). The authors show that TAMs in SCC are heterogeneously activated, exhibiting both M1 and M2 states of activation, and that macrophages can simultaneously express genes commonly associated with Th1 and Th2 responses (24). To further investigate TAM phenotypes *in vivo*, we obtained SCCs

tumors (n=3) and peri-tumoral normal skin samples (n=3) from the same patients. This served a control for TAMS as tissue resident macrophages can have varied phenotypic characteristics depending on their tissue niche. Dermal macrophages from the same patient are the ideal control for immunophenotype characterization of TAMs *in vivo* in human SCCs. The results demonstrate that TAMs in SCCs are M1 and M2 activated and also express high MMP-9 levels compared to skin-resident macrophages (Figure 5).

The simple categorization of macrophages into M1 and M2 phenotypes does not capture the observed complexity of TAM activation in SCC microenvironment. Therefore, a revised model of macrophage activation states taking into account the shades and overlaps of activations states known as the color wheel of macrophage activation is more appropriate in explaining the *in vivo* behavior of macrophages (20, 32). In this model, macrophages are divided into three populations: classically activated macrophages, wound-healing macrophages, and immune regulatory ones, while allowing for overlap of these three states on a color wheel (20, 32). The phenotypic complexity of TAMs is possibly due to heterogeneity of the tumor microenvironment ranging from hypoxic and necrotic regions to more vascularized regions; In addition, infiltration by a variety of T cells, IFN-gamma producing Th1, IL-4 and IL-13 producing Th2 cells and IL-10 producing T-reg cells results in a heterogeneous cytokine milieu in the tumor microenvironment. In support of this hypothesis, it has been shown that SCC is associated with a mixed Th1 and Th2 gene expression profile (33). In addition, It is important to note that the monocyte lineage, the precursor to TAMs and tissue-resident macrophages, are themselves heterogeneous, yet providing another potential factor that mediates the diverse phenotypic characteristic of TAMs (34). In addition, tumor cells in

SCC and BCC can produce cytokines such as IL-10 further contributing to the diverse nature of chemical messages in the tumor niche (35).

Higher MMP-9 and arginase I Expression in TAMs in SCCs *versus* BCCs

MMPs are a family of zinc-dependent neutral endopeptidases that can break down the components of the extracellular matrix (ECM) (36). MMPs play an active role in many aspects of tumor development including angiogenesis, local tissue invasion, and metastasis (37). The ECM is a net of connective tissue that stands in the way of tumor growth and invasion. When tumor cells are embedded in this rigid, spheroid matrix, tumor proliferation is suspended (38). In addition to tumor proliferation, MMPs allow tumor cells to locally invade and metastasize through vascular and lymphatic pathways through breakdown of basement membrane proteins (39, 40). Macrophages are known to produce matrix metalloproteinase, primarily MMP-9 and MMP-2 and can contribute to tumor growth, invasion and metastasis by supplying this pivotal factor in the tumor microenvironment (22, 23).

Increased expression of MMP-9 in TAMs from SCCs as compared with BCCs is an interesting finding that suggests a possible reason for the difference in clinical behavior between SCC and BCC (Figure 2). MMP-9 supplied by bone marrow-derived cells has been shown to be involved in skin carcinogenesis (41). A murine model of HPV16-induced *de novo* SCC demonstrated that MMP-9 knock out mice have reduced keratinocyte proliferation and delayed progression from hyperplasia to dysplasia and finally to invasive carcinoma (41). In a similar manner, immunohistochemical studies of MMP-9 and collagen IV, one of the known substrates of MMP-9, revealed that SCC has

increased expression of MMP-9 and MMP-2 and decreased collagen IV when compared to BCC (42). Given this essential role of MMP-9 in skin carcinogenesis, increased MMP-9 produced by TAMs in SCC *versus* BCC can partly explain the clinical behavior of these two tumor types.

Arginase I is a key enzyme that is involved in polyamine production (putrescine, spermine, spermidine). Arginase I converts Arginine to Ornithine, which is subsequently converted to putrescine by Ornithine Decarboxylase (ODC). Putrescine is then interconverted to other polyamines through the actions of spermidine synthase and spermine synthase (43). This biochemical pathway leads to production of polyamines in the tumor niche, which can then be utilized by tumor cells for cellular proliferation and growth (44). The distinctly higher levels of arginase I in TAMs from SCCs *versus* BCCs may be a pathophysiologic reason for the higher growth rates observed in SCC as compared to BCC (Figure 2). Finally, higher expression of arginase I in TAMs from SCCs also demonstrates that there are more M2, tumor-promoting macrophages present in SCCs as compared to BCCs.

Soluble factors are sufficient to reproduce the TAM immunophenotype

Co-culture of human cutaneous SCC with THP-1 cells demonstrated that cells in the tumor microenvironment are able to induce M1 and M2 polarization in macrophages *in vitro* through non-contact-dependent, paracrine communication (Figure 6). The fact that normal skin from the same patient does not induce the phenotype demonstrates that the soluble factor(s) are present in the tumor and absent from adjacent "normal" tissue. This is similar to our *in vivo* FACS immunophenotype of TAMs in SCCs, which shows

heterogeneous M1 and M2 activation and increased MMP-9 production as compared to peri-tumoral normal skin and BCC (Figure 2 and 5). Increased MMP-9 production in THP-1 cells as a result of co-culture with SCCs is also consistent with our *in vivo* results of TAMs in SCCs.

The possible mechanism of TAM immunophenotype induction is through soluble factor(s) that are responsible for induction of TAM immunophenotype (Figure 7). The source of such signaling factors can include tumor cells, Th1 and Th2 cells, other immune cells, fibroblasts, and variety of other cells in the tumor microenvironment. In support of this hypothesis, we demonstrated that THP-1 cells could be induced to their respective M1-M2 phenotype *in* vitro using filtered (cell-free) tumor-conditioned media from SCCs and BCCs (Figure 7). The results show a stepwise increase in mean florescent intensity from THP-1 cells incubated with control media to the BCC-conditioned media to the SCC-conditioned media (Figure 7). In summary, the results of both SCC and peri-tumoral normal skin co-culture with THP-1 cells together with *in vitro* THP-1 cell polarization with SCC-conditioned and BCC-conditioned media further support the *in vivo* FACS immunophenotype of TAMs isolated from NMSC (Figure 2, 6, and 7). Given the heterogeneity and complexity of the tumor niche, monocytes recruited into the tumor microenvironment are exposed to a multitude of factors. Based on our findings, the heterogeneous, multi-focal activation is most likely the result of multiple soluble factors that act through a paracrine, non-contact-dependent relationship to induce an intricate phenotype in TAMs that involves features of both M1 and M2 activation.

Imiquimod induces M1 activation of TAMs *in vivo* and *in vitro*

TAMs have been described as as a double-edged sword in cancer biology (45). It is important to understand their multifaceted behavior in order to devise ways to alter their activation state as a therapy for cancer. It is known that TAMs are dynamic and can be polarized into different activation states through exposure to different cytokines and immunomodulators (21, 23, 46). Given the broad role of TAMs in a variety of malignancies, it is conceivable that macrophage-targeted therapies will be useful for numerous cancers. Both imiquimod and resiquimod have been shown to be immunomodulators of T cells through the enhancement of Th1 cells and IFN-gamma production (47). Clinically, treatment of superficial BCC with 5 % imiquimod leads to significant increase in infiltrating CD68+ macrophages compared to baseline (48). Similarly, treatment of actinic keratoses (AK) with imiquimod leads to increase in gene expression of macrophage markers (CD163, CD14, CLECSF9) and activated T cells including cytotoxic T cells and Th1 cells (49). The increased infiltration of macrophages into BCCs and AKs after treatment with imiquimod has significant implications in terms of the mechanism of imiquimod's tumoricidal action. We analyzed published microarray data of up-regulated genes in BCCs (n=36) after topical imiquimod therapy. Ten known M1 genes are up-regulated through imiquimod treatment including CD40, CCR7, CD86, STAT1, MX-1, CXCL9, CXCL10, CCL2, CCL3, and CCL4 (Supplementary Figure 1) (50).

We sought to determine the state of polarization of TAMs *in vivo* in response to imiquimod treatment using flow cytometric immunophenotyping of SCCs as compared to SCC controls. We found that imiquimod treatment of SCCs leads to strong M1 activation

of TAMs as shown by increased levels of CD40 and CD127 as compared to control SCCs (Figure 9). Similarly, *in vitro* stimulation of THP-1 cells with imiquimod and resiquimod induced M1 activation as well (Figure 8). From a mechanistic viewpoint, M1 macrophages are known to have potent tumoricidal properties mediated by production of pro-inflammatory factors (51). Given that Th1 cell are induced by imiquimod, one of the contributors to M1 polarization of macrophages by imiquimod is possibly through Th1 production of IFN-gamma (21). Interestingly, using imiquimod alone, we showed that strong M1 activation could be reproduced with human monocytic cell lines in the absence of T cells and other cytokines (Figure 8). Therefore, imiquimod and resiquimod are sufficient to attenuate macrophage polarization without the need of adaptive immune cells. Imiquimod is known to be a TLR-7/8 agonist and this maybe the mechanism of M1 polarization that we have observed *in vivo* and *in vitro* (52).

Imiquimod is an immunomodulator of macrophages

The results in Figure 10 provide insight into a novel mechanism of imiquimod's action that we subsequently studied further using *in vitro* experiments to model the tumor microenvironment. We obtained tumor-conditioned media through manual dissociation of Mohs debulked tumors incubated in complete media for 24 hours and which we then filtered in a sterile fashion. Next, we polarized THP-1 cells in presence or absence of imiquimod to study effects on macrophage polarization. Imiquimod leads to strong M1 polarization and simultaneous reduction in both M2 polarization and MMP-9 production (Figure 10). These findings imply that under conditions that model the microenvironment of BCCs and SCCs, imiquimod can override these states of TAM polarization, resulting

in a high M1 and low M2 polarized state. This modulated state of polarization is markedly distinct from the TAM immunophenotype that we have shown *in vivo* and *in vitro* and provides insight to a potential mechanism of imiquimod. The other implication is that TAMs in human tumors exhibit plasticity and can be modulated through both amplification of their tumoricidal effects and attenuation of their tumor-promoting functions. TAMs provide a continual supply of growth factors, angiogenic factors and MMPs that contribute to growth, invasion, and metastasis of tumor cells (3, 53). Macrophage immunomodulators may be useful across a variety of tumor types as TAMs are present in numerous types of tumors.

Imiquimod-primed macrophages induce apoptosis of tumor cells and demonstrate enhanced phagocytosis of epidermoid carcinoma cells

We asked question of whether imiquimod can induce macrophage to display tumoricidal activity. We specifically focused on apoptosis of tumor cells and phagocytosis of tumor cells by macrophages. In our apoptosis experiments, imiquimod-primed macrophages induced apoptosis of epidermoid carcinoma cells at a level six-fold greater than naïve macrophages (Figure 11). This was carried out in a non-contact dependent co-culture system. The results demonstrate that imiquimod can induce macrophages to exhibit tumoricidal activity through the secretion of soluble cytotoxic factors that can cause both early and late apoptosis in carcinoma cells (Figure 11). Given that M1 macrophages are known for their pro-inflammatory activity against infectious agents, we speculate that imiquimod causes macrophages to polarize to an M1, pro-inflammatory state, which results in the secretion of cytotoxic factors such as tumor

necrosis factor (TNF), Nitric Oxide (NO), and reactive oxygen species leading to increased apoptosis of tumor cells (51).

We devised a phagocytosis assay utilizing PE-labeled epidermoid carcinoma cells and THP-1 macrophages primed with imiquimod to investigate whether imiquimod enhances the phagocytic activity of macrophages. In a contact system, tumor cells labeled with PE were incubated in suspension with control and imiquimod primed macrophages. Interestingly, imiquimod primed macrophages had significantly enhanced phagocytic activity. The rate of phagocytosis of PE-labeled tumor cells was 68.2 % in the imiquimod primed macrophage group compared to 8.22 % in the control macrophage group (Figure 12). The results of these experiments demonstrate that imiquimod can activate tumoricidal activity of macrophages as shown by both enhanced apoptosis and phagocytosis of tumor cells by imiquimod-activated macrophages.

In conclusion, using a novel method of FACS immunophenotyping of SCC and BCC tumor cells, we have shown that TAMs in human cutaneous SCCs show a heterogeneous M1 and M2 activation state. TAMs in SCCs express significantly higher levels of M1 (CD40, CD127) and M2 (arginase I) markers as compared to BCCs and also express higher levels of MMP-9, a pivotal factor in ECM remodeling and tumor invasion (36, 38, 39). SCC, a relatively aggressive human skin cancer, is able to induce a more highly polarized TAM population, which is capable of both tumor-promoting functions (M2, MMP-9) and tumor-inhibiting functions (M1) in vivid contrast to the more indolent skin cancer, BCC. These findings demonstrate that TAMs may play an important role in pathophysiology of NMSC, the most common cancers in humans. Future studies include the characterization of how the M1/M2 heterogeneity of TAMs is maintained in the

tumor microenvironment and also in the identification of soluble macrophage modulators.

Further, we demonstrated that imiquimod, a TLR-7 agonist approved by the FDA for the treatment of superficial BCC, is able to induce M1 polarization in TAMs from human SCC and can induce the same phenotype *in vitro*. Further, imiquimod directly induces M1 polarization and suppresses M2 polarization in a tumor microenvironment assay. In functional assay, we demonstrated that activates macrophages to both induce apoptosis and phagocytosis of carcinoma cells.

Taken together, these results suggest a mechanism by which imiquimod activates TAMs to an M1 polarized state capable of induction of apoptosis and phagocytosis of tumor cells. These results reveal a novel immunologic mechanism for imiquimod in the treatment of skin cancer and suggest that modulation of TAM immunophenotype may be a therapeutic strategy useful in the treatment of numerous cancers.

Table A - Characteristic of Subjects and tumor specimens

	Type	Age	Gender	Duration of lesion	Tumor size (cm)	Location	Skin CA history
1	BCC	54	M	2 years	1.8 x 1.8	L to midline mid back	none
2	SCC	58	M	6 months	1.2 x 1.2	L temple	Infitrative BCC, SCC, BCCs
3	SCC	100	M	6 months	2.5 x 2.5	L radial hand	BCC, SCC
4	SCC	98	F	3 months	2.0 x 2.5	L cheek	SCC
5	BCC, Micronodular	71	M	2 years	0.4 x 0.5	L forehead	none
6	SCC	95	F	3 months	2.0 x 1.8	R nasal bulb	SCC
7	BCC	78	M	6 months	1.2 x 1.0	L inferior eyelid	none
8	BCC	77	M	1 year	1.5 x 1.1	L side of nose	BCC, SCCis, malignant melanoma
9	BCC, nodular and infiltrating	76	M	6 months	1.0 x 1.2	L zygoma	BCC
10	SCC	49	M	6 months	0.8 x 0.9	L cheek	SCCis, Aks, SCC, BCC
11	SCC, Invasive SCC to base	85	M	3 months	0.9 x 0.8	L ear	none
12	SCC	81	M	6 months	1.0 x 1.2	R inferior cheek	BCC
13	SCC	96	F	6 months	1.8 x 2.3	R medial cheek	none
14	SCC	65	M	3 months	1.3 x 1.4	Frontal Scalp	SCC, BCC
15	SCC	51	M	6 months	1.3 x 0.9, 1.0 x 1.5	L preauricular, L Scalp	Invasive SCCs, Aks
16	BCC- to base	66	M	6 months	0.7 x 0.7	R nose	none
17	SCC	78	M	1 month	1.3 x 1.3	L forehead	none
18	SCC, Peri-tumoral skin	83	M	2 months	2.6 x 3.4	R cheek	SCC
19	SCC	85	M	3 months	1.3 x 1.4	R distal shin	AK, BCC
20	SCC	92	F	3 months	2.0 x 2.0	L mid anterior leg	AK
21	BCC with infiltrative features	63	M	10 years	3.5 x 2.4	L chest	none
22	SCC	83	F	3 months	0.8 x 0.8	L cheek	none
23	BCC	87	F	5 years	3.0 x 3.0	Back	none
24	SCC	91	F	1 year	1.0 x 1.0	R lower cheek	SCCis, Atypical nevus
25	SCC, Peri-tumoral skin	67	M	6 months	2.5 x 2.4	R temple	none

Abbreviations: M- Male, F- Female, L- Left, R- Right, SCC- Squamous Cell Carcinoma, BCC- Basal Cell Carcinoma, SCCis- Squamous cell carcinoma-in situ, AK- Actinic Keratosis

REFERENCES

1. Coussens, L.M., and Werb, Z. 2002. Inflammation and cancer. *Nature* 420:860-867.

2. Mantovani, A., Sozzani, S., Locati, M., Allavena, P., and Sica, A. 2002. Macrophage polarization: tumor-associated macrophages as a paradigm for polarized M2 mononuclear phagocytes. *Trends Immunol* 23:549-555.

3. Pollard, J.W. 2004. Tumour-educated macrophages promote tumour progression and metastasis. *Nat Rev Cancer* 4:71-78.

4. Grivennikov, S.I., Greten, F.R., and Karin, M. 2010. Immunity, inflammation, and cancer. *Cell* 140:883-899.

5. van Ravenswaay Claasen, H.H., Kluin, P.M., and Fleuren, G.J. 1992. Tumor infiltrating cells in human cancer. On the possible role of CD16+ macrophages in antitumor cytotoxicity. *Lab Invest* 67:166-174.

6. Karin, M., and Greten, F.R. 2005. NF-kappaB: linking inflammation and immunity to cancer development and progression. In *Nat Rev Immunol*. England. 749-759.

7. Qian, B.Z., and Pollard, J.W. 2010. Macrophage diversity enhances tumor progression and metastasis. In *Cell*. United States: 2010 Elsevier Inc. 39-51.

8. Wyckoff, J.B., Wang, Y., Lin, E.Y., Li, J.F., Goswami, S., Stanley, E.R., Segall, J.E., Pollard, J.W., and Condeelis, J. 2007. Direct visualization of macrophage-assisted tumor cell intravasation in mammary tumors. In *Cancer Res*. United States. 2649-2656.

9. Alam, M., and Ratner, D. 2001. Cutaneous squamous-cell carcinoma. *N Engl J Med* 344:975-983.

10. Lomas, A., Leonardi-Bee, J., and Bath-Hextall, F. 2012. A systematic review of worldwide incidence of nonmelanoma skin cancer. *Br J Dermatol* 166:1069-1080.

11. Neville, J.A., Welch, E., and Leffell, D.J. 2007. Management of nonmelanoma skin cancer in 2007. In *Nat Clin Pract Oncol*. England. 462-469.

12. Miller, D.L., and Weinstock, M.A. 1994. Nonmelanoma skin cancer in the United States: incidence. *J Am Acad Dermatol* 30:774-778.

13. Madan, V., Lear, J.T., and Szeimies, R.M. 2010. Non-melanoma skin cancer. *Lancet* 375:673-685.

14. Miller, S.J. 1991. Biology of basal cell carcinoma (Part I). *J Am Acad Dermatol* 24:1-13.

15. Miller, S.J. 1991. Biology of basal cell carcinoma (Part II). *J Am Acad Dermatol* 24:161-175.

16. Benjamin, C.L., and Ananthaswamy, H.N. 2007. p53 and the pathogenesis of skin cancer. In *Toxicol Appl Pharmacol*. United States. 241-248.

17. Kang, K., Hammerberg, C., Meunier, L., and Cooper, K.D. 1994. CD11b+ macrophages that infiltrate human epidermis after in vivo ultraviolet exposure potently produce IL-10 and represent the major secretory source of epidermal IL-10 protein. *J Immunol* 153:5256-5264.

18. Tjiu, J.W., Chen, J.S., Shun, C.T., Lin, S.J., Liao, Y.H., Chu, C.Y., Tsai, T.F., Chiu, H.C., Dai, Y.S., Inoue, H., et al. 2009. Tumor-associated macrophage-

induced invasion and angiogenesis of human basal cell carcinoma cells by cyclooxygenase-2 induction. *J Invest Dermatol* 129:1016-1025.

19. Moussai, D., Mitsui, H., Pettersen, J.S., Pierson, K.C., Shah, K.R., Suárez-Fariñas, M., Cardinale, I.R., Bluth, M.J., Krueger, J.G., and Carucci, J.A. 2011. The human cutaneous squamous cell carcinoma microenvironment is characterized by increased lymphatic density and enhanced expression of macrophage-derived VEGF-C. *J Invest Dermatol* 131:229-236.

20. Mosser, D.M. 2003. The many faces of macrophage activation. *J Leukoc Biol* 73:209-212.

21. Mantovani, A., Sica, A., and Locati, M. 2005. Macrophage polarization comes of age. In *Immunity*. United States. 344-346.

22. Sica, A., Schioppa, T., Mantovani, A., and Allavena, P. 2006. Tumour-associated macrophages are a distinct M2 polarised population promoting tumour progression: potential targets of anti-cancer therapy. *Eur J Cancer* 42:717-727.

23. Sica, A., and Mantovani, A. 2012. Macrophage plasticity and polarization: in vivo veritas. *J Clin Invest* 122:787-795.

24. Pettersen, J.S., Fuentes-Duculan, J., Suarez-Farinas, M., Pierson, K.C., Pitts-Kiefer, A., Fan, L., Belkin, D.A., Wang, C.Q., Bhuvanendran, S., Johnson-Huang, L.M., et al. 2011. Tumor-associated macrophages in the cutaneous SCC microenvironment are heterogeneously activated. In *J Invest Dermatol*. United States. 1322-1330.

25. Biswas, S.K., and Mantovani, A. 2010. Macrophage plasticity and interaction with lymphocyte subsets: cancer as a paradigm. *Nat Immunol* 11:889-896.

26. Urosevic, M., Maier, T., Benninghoff, B., Slade, H., Burg, G., and Dummer, R. 2003. Mechanisms underlying imiquimod-induced regression of basal cell carcinoma in vivo. *Arch Dermatol* 139:1325-1332.

27. Jurk, M., Heil, F., Vollmer, J., Schetter, C., Krieg, A.M., Wagner, H., Lipford, G., and Bauer, S. 2002. Human TLR7 or TLR8 independently confer responsiveness to the antiviral compound R-848. *Nat Immunol* 3:499.

28. Fishelevich, R., Zhao, Y., Tuchinda, P., Liu, H., Nakazono, A., Tammaro, A., Meng, T.C., Lee, J., and Gaspari, A.A. 2011. Imiquimod-induced TLR7 signaling enhances repair of DNA damage induced by ultraviolet light in bone marrow-derived cells. *J Immunol* 187:1664-1673.

29. Brown, B.N., Valentin, J.E., Stewart-Akers, A.M., McCabe, G.P., and Badylak, S.F. 2009. Macrophage phenotype and remodeling outcomes in response to biologic scaffolds with and without a cellular component. In *Biomaterials*. England. 1482-1491.

30. Badylak, S.F., Valentin, J.E., Ravindra, A.K., McCabe, G.P., and Stewart-Akers, A.M. 2008. Macrophage phenotype as a determinant of biologic scaffold remodeling. *Tissue Eng Part A* 14:1835-1842.

31. Riker, A.I., Enkemann, S.A., Fodstad, O., Liu, S., Ren, S., Morris, C., Xi, Y., Howell, P., Metge, B., Samant, R.S., et al. 2008. The gene expression profiles of primary and metastatic melanoma yields a transition point of tumor progression and metastasis. *BMC Med Genomics* 1:13.

32. Mosser, D.M., and Edwards, J.P. 2008. Exploring the full spectrum of macrophage activation. In *Nat Rev Immunol*. England. 958-969.

33. Kosmidis, M., Dziunycz, P., Suárez-Fariñas, M., Mühleisen, B., Schärer, L., Läuchli, S., Hafner, J., French, L.E., Schmidt-Weber, C., Carucci, J.A., et al. 2010. Immunosuppression affects CD4+ mRNA expression and induces Th2 dominance in the microenvironment of cutaneous squamous cell carcinoma in organ transplant recipients. *J Immunother* 33:538-546.

34. Gordon, S., and Taylor, P.R. 2005. Monocyte and macrophage heterogeneity. In *Nat Rev Immunol*. England. 953-964.

35. Kim, J., Modlin, R.L., Moy, R.L., Dubinett, S.M., McHugh, T., Nickoloff, B.J., and Uyemura, K. 1995. IL-10 production in cutaneous basal and squamous cell carcinomas. A mechanism for evading the local T cell immune response. *J Immunol* 155:2240-2247.

36. Johansson, N., Ahonen, M., and Kahari, V.M. 2000. Matrix metalloproteinases in tumor invasion. *Cell Mol Life Sci* 57:5-15.

37. Kerkela, E., and Saarialho-Kere, U. 2003. Matrix metalloproteinases in tumor progression: focus on basal and squamous cell skin cancer. In *Exp Dermatol*. Denmark. 109-125.

38. Hotary, K.B., Allen, E.D., Brooks, P.C., Datta, N.S., Long, M.W., and Weiss, S.J. 2003. Membrane type I matrix metalloproteinase usurps tumor growth control imposed by the three-dimensional extracellular matrix. In *Cell*. United States. 33-45.

39. Deryugina, E.I., and Quigley, J.P. 2006. Matrix metalloproteinases and tumor metastasis. *Cancer Metastasis Rev* 25:9-34.

40. Fingleton, B. 2006. Matrix metalloproteinases: roles in cancer and metastasis. In *Front Biosci*. United States. 479-491.

41. Coussens, L.M., Tinkle, C.L., Hanahan, D., and Werb, Z. 2000. MMP-9 supplied by bone marrow-derived cells contributes to skin carcinogenesis. In *Cell*. United States. 481-490.

42. Dumas, V., Kanitakis, J., Charvat, S., Euvrard, S., Faure, M., and Claudy, A. 1999. Expression of basement membrane antigens and matrix metalloproteinases 2 and 9 in cutaneous basal and squamous cell carcinomas. *Anticancer Res* 19:2929-2938.

43. Das, P., Lahiri, A., and Chakravortty, D. 2010. Modulation of the arginase pathway in the context of microbial pathogenesis: a metabolic enzyme moonlighting as an immune modulator. *PLoS Pathog* 6:e1000899.

44. Gerner, E.W., and Meyskens, F.L. 2004. Polyamines and cancer: old molecules, new understanding. *Nat Rev Cancer* 4:781-792.

45. Chen, J.J., Lin, Y.C., Yao, P.L., Yuan, A., Chen, H.Y., Shun, C.T., Tsai, M.F., Chen, C.H., and Yang, P.C. 2005. Tumor-associated macrophages: the double-edged sword in cancer progression. In *J Clin Oncol*. United States. 953-964.

46. Mantovani, A., Sica, A., and Locati, M. 2007. New vistas on macrophage differentiation and activation. *Eur J Immunol* 37:14-16.

47. Smith, K.J., Hamza, S., and Skelton, H. 2004. Topical imidazoquinoline therapy of cutaneous squamous cell carcinoma polarizes lymphoid and monocyte/macrophage populations to a Th1 and M1 cytokine pattern. In *Clin Exp Dermatol*. England. 505-512.

48. Vidal, D., Matías-Guiu, X., and Alomar, A. 2004. Open study of the efficacy and mechanism of action of topical imiquimod in basal cell carcinoma. *Clin Exp Dermatol* 29:518-525.

49. Torres, A., Storey, L., Anders, M., Miller, R.L., Bulbulian, B.J., Jin, J., Raghavan, S., Lee, J., Slade, H.B., and Birmachu, W. 2007. Immune-mediated changes in actinic keratosis following topical treatment with imiquimod 5% cream. *J Transl Med* 5:7.

50. Panelli, M.C., Stashower, M.E., Slade, H.B., Smith, K., Norwood, C., Abati, A., Fetsch, P., Filie, A., Walters, S.A., Astry, C., et al. 2007. Sequential gene profiling of basal cell carcinomas treated with imiquimod in a placebo-controlled study defines the requirements for tissue rejection. *Genome Biol* 8:R8.

51. Murray, P.J., and Wynn, T.A. 2011. Protective and pathogenic functions of macrophage subsets. *Nat Rev Immunol* 11:723-737.

52. Schön, M.P., and Schön, M. 2007. Imiquimod: mode of action. *Br J Dermatol* 157 Suppl 2:8-13.

53. Pollard, J.W. 2009. Trophic macrophages in development and disease. *Nat Rev Immunol* 9:259-270.

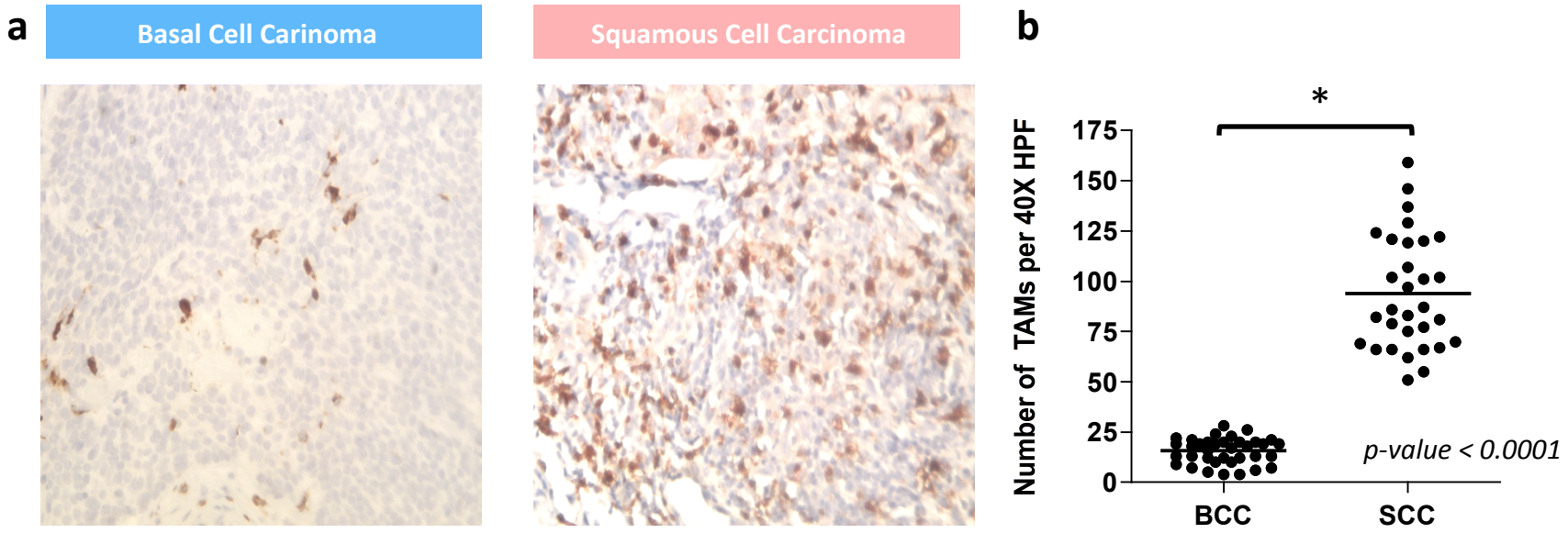

Figure 1 Higher density of CD68+ tumor-associated macrophages are found in cutaneous SCC as compared to BCC

(**a**) BCCs (n=6) and SCCs (n=5) were stained with CD68 antibody, a marker of tumor-associated macrophages (TAMs) and visualized at 40X.

(**b**) Number of CD68+ TAMs was counted in six high power fields (HPF) for each BCC and SCC using Optiphot Nikon microscope with camera. Number of TAMs per HPF in SCC is significantly higher than BCC as shown in this graph (* p-value < 0.0001, unpaired t test)

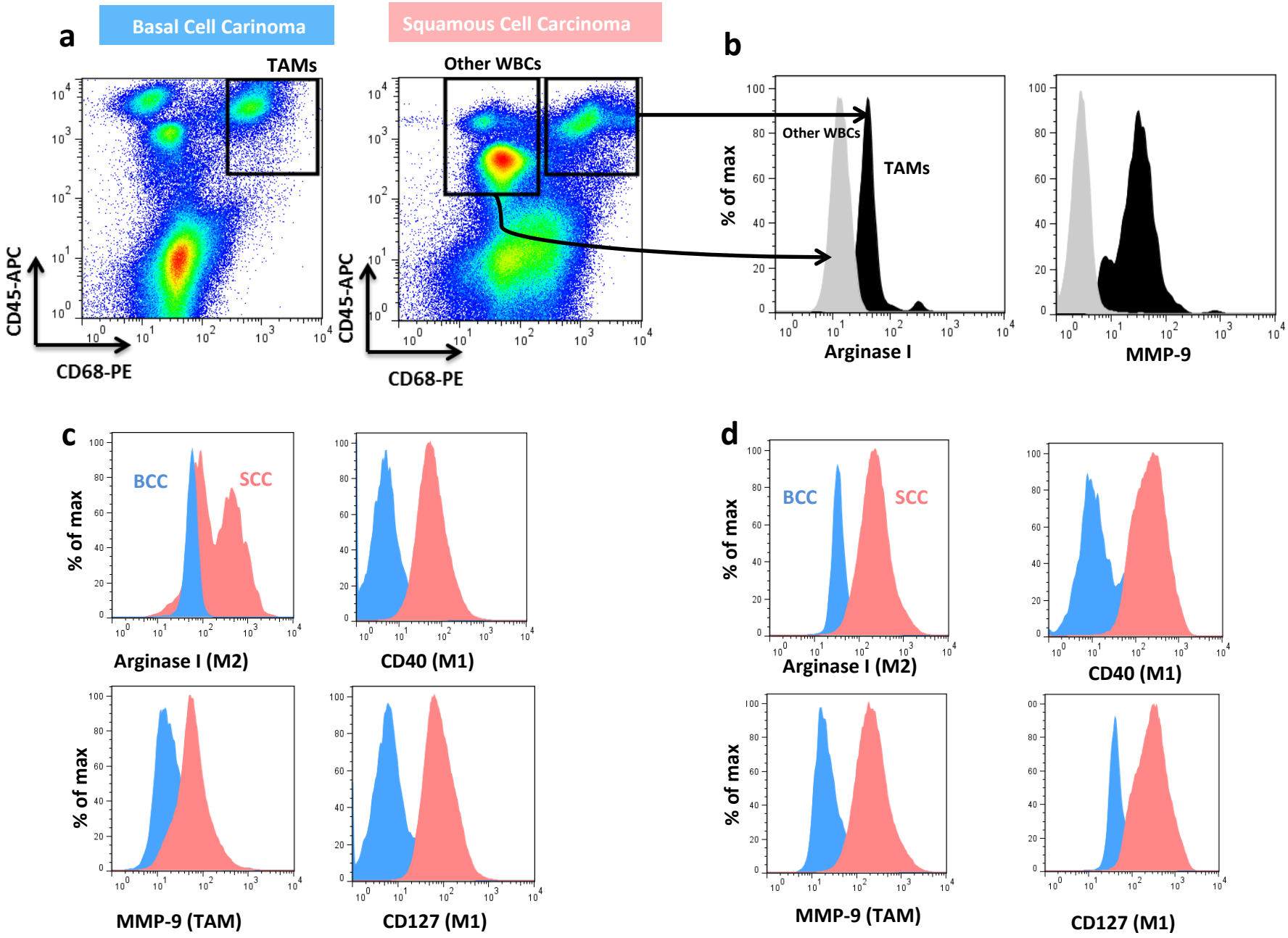
a
Basal Cell Carinoma
Squamous Cell Carcinoma
TAMs
Other WBCs
CD45-APC
CD68-PE
b
Other WBCs
TAMs
% of max
Arginase I
MMP-9
c
BCC
SCC
% of max
Arginase I (M2)
CD40 (M1)
MMP-9 (TAM)
CD127 (M1)
d
BCC
SCC
% of max
Arginase I (M2)
CD40 (M1)
MMP-9 (TAM)
CD127 (M1)

Figure 2 Tumor-associated macrophages in SCC and BCC show differential activation based on flow cytometric immunophenotype of M1 and M2 markers

(**a**) SCCs (n=7) and BCCs (n=7) excised using Mohs were enzymatically dissociated with Liberase for flow cytometric immunophenotyping. CD68-PE and CD45-APC were utilized as macrophage marker and common leukocyte marker respectively. As seen on this FACS plot, CD68+CD45+ population was gated upon as TAMs. CD68-CD45+ were gated upon to represent other white blood cells (other WBCs). The CD68-CD45- population seen in these plots represents tumor cells and other non-hematopoietic cell types in the tumor microenvironment.
(**b**) Histograms of MMP-9 and arginase I were created for TAMs (CD68+CD45+), shown in black, and other WBCs (CD68+CD45-), shown in grey. The resulting overlayed histograms show that MMP-9 and arginase-I have higher levels in TAMs as compared to other WBCs.
(**c**) CD68+CD45+ TAMs in SCC and BCC were gated upon. Histograms of arginase-I, MMP-9, CD40, and CD127 were created and overlayed for comparison of TAM immunophenotype in SCC (red) vs. BCC (blue). Characterization of M1, pro-inflammatory surface markers shows that TAMs in SCC have higher levels of CD40 and CD127 compared to BCC. Characterization of MMP-9 and Arginase-I, which are markers of tumor-promoting TAMs, shows that TAMs in SCC microenvironment have higher levels of both markers as shown by noticeable histogram shifts in these plots.
(**d**) CD163+CD68+ TAMs in SCC have higher levels of M1 (CD40, CD127), arginase I, and MMP-9 as compared to CD163+CD68+ TAMs in BCC as shown by histogram shifts.

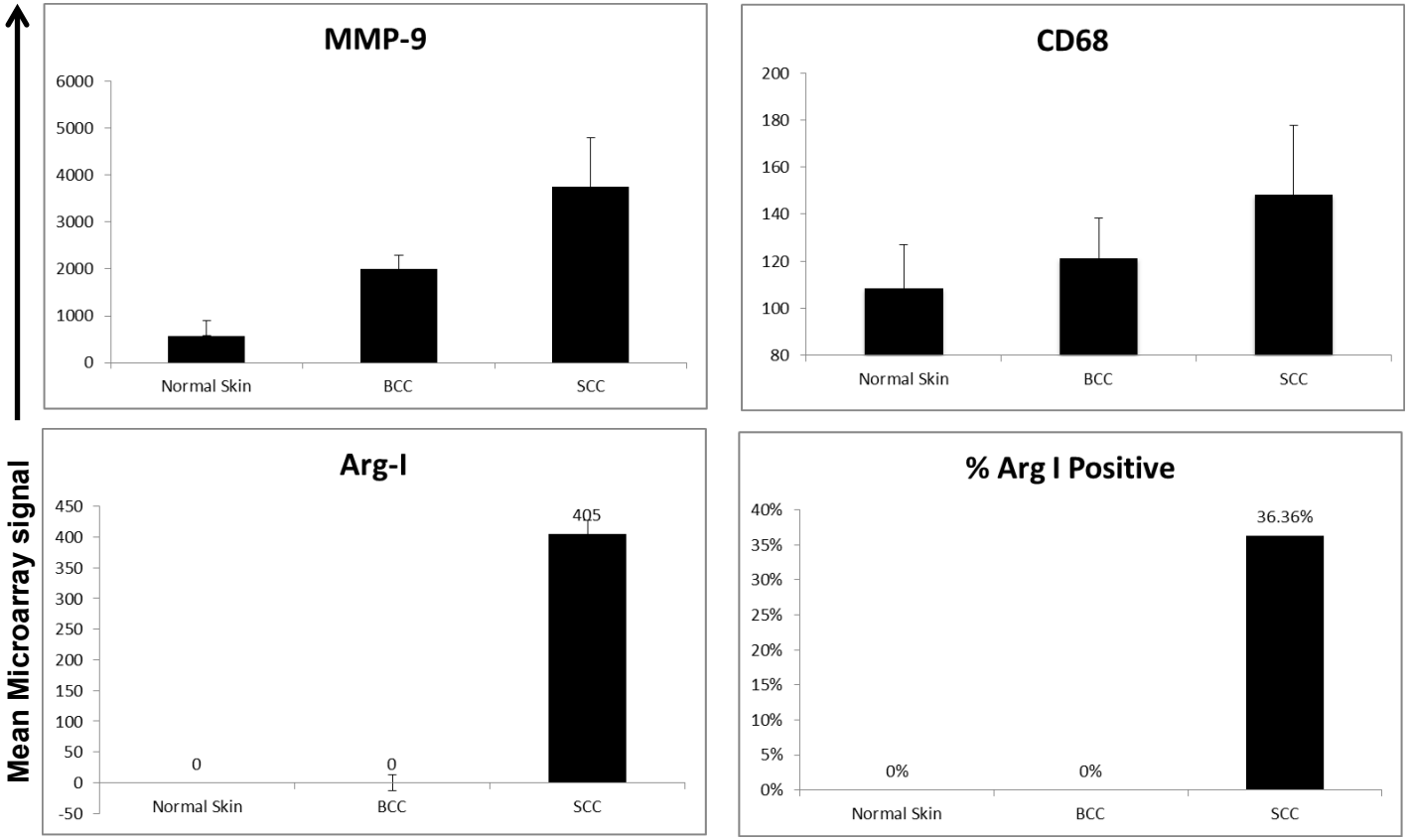

Figure 3 Microarray of Human SCC and BCC shows differential expression of CD68, MMP-9, and arginase-I

Whole tumor microarrays of human SCCs (n=13) and BCCs (n=11) and normal skin (n=4) from published data were utilized to calculated microarray signal density for MMP9, CD68, and arginase-I. MMP-9 expression is higher in SCC compared to BCC, which are both higher than normal skin. Similarly, CD68, a classic macrophage marker shows higher levels of expression in SCC compared to BCC and normal skin. Arginase I shows high expression in SCC, but no expression in BCC or normal skin. % arginase I positive is defined as percentage of all samples with significant p-values indicating that the gene expression is present in microarray profile of the tumor. SCC shows 36.36 % of arginase I positivity whereas BCC and normal skin demonstrate 0 % arginase I positivity.
Abbreviations: Arg-I (arginase I)

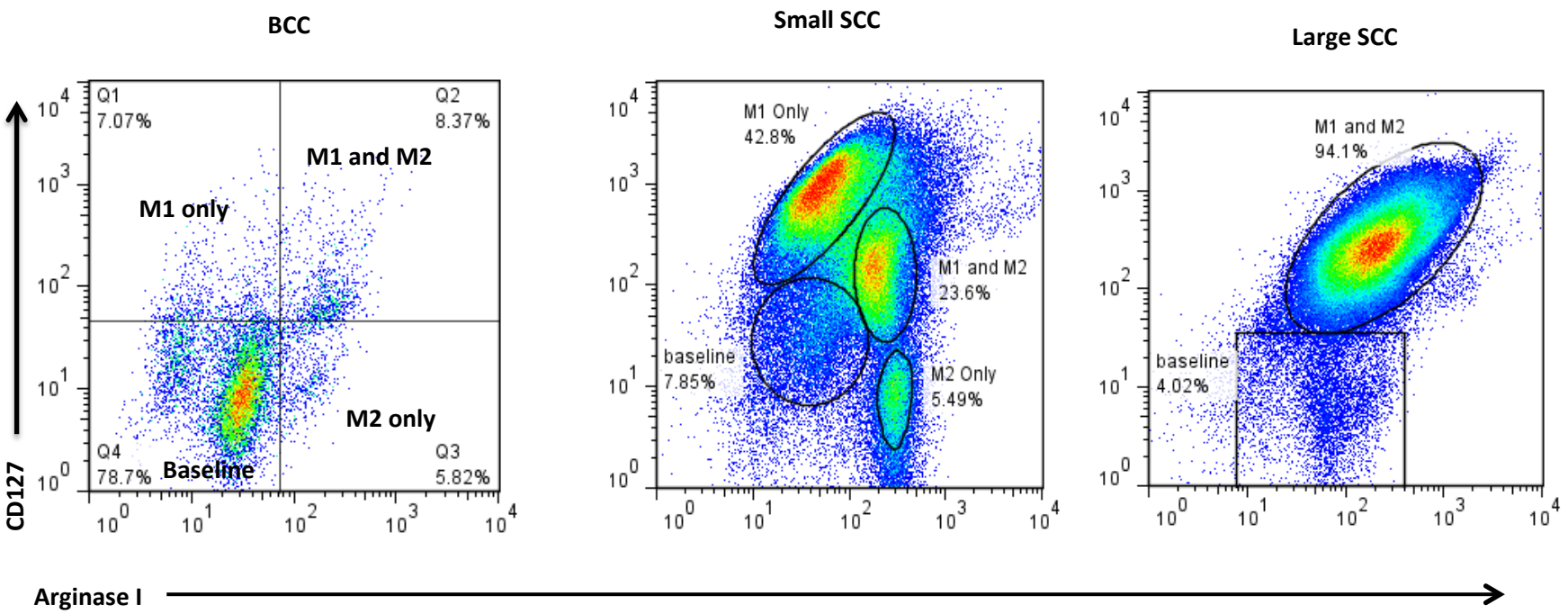

Figure 4 Subpopulation analysis of SCC and BCC tumor-associated macrophages demonstrates heterogeneous states of macrophage polarization

M1 vs. M2 graphs were created for CD68+CD45+ cells using CD127 (M1) vs. arginase-1 (M2) plots. In BCC, 78.7 % of TAMs have baseline level of activation (78.7 %), M1 only activation (7.07 %), M2 only activation (5.82 %), and M1-M2 activation (8.37 %). In contrast, in a small SCC, 7.85 % of TAMs have baseline activation (7.85 %), 42.8 % M1 only (42.8 %), M2 only (5.49 %), and M1-M2 activation (23.6 %). In large SCC, majority of TAMs have M1-M2 activation (94.1 %) and a small percentage have baseline activation (4.02 %). The results suggest that TAMs in SCC have heterogeneous M1-M2 immunophenotype compared to BCC. In BCC, majority of TAMs are quiescent whereas in SCC most TAMs have a heterogeneous state of polarization.

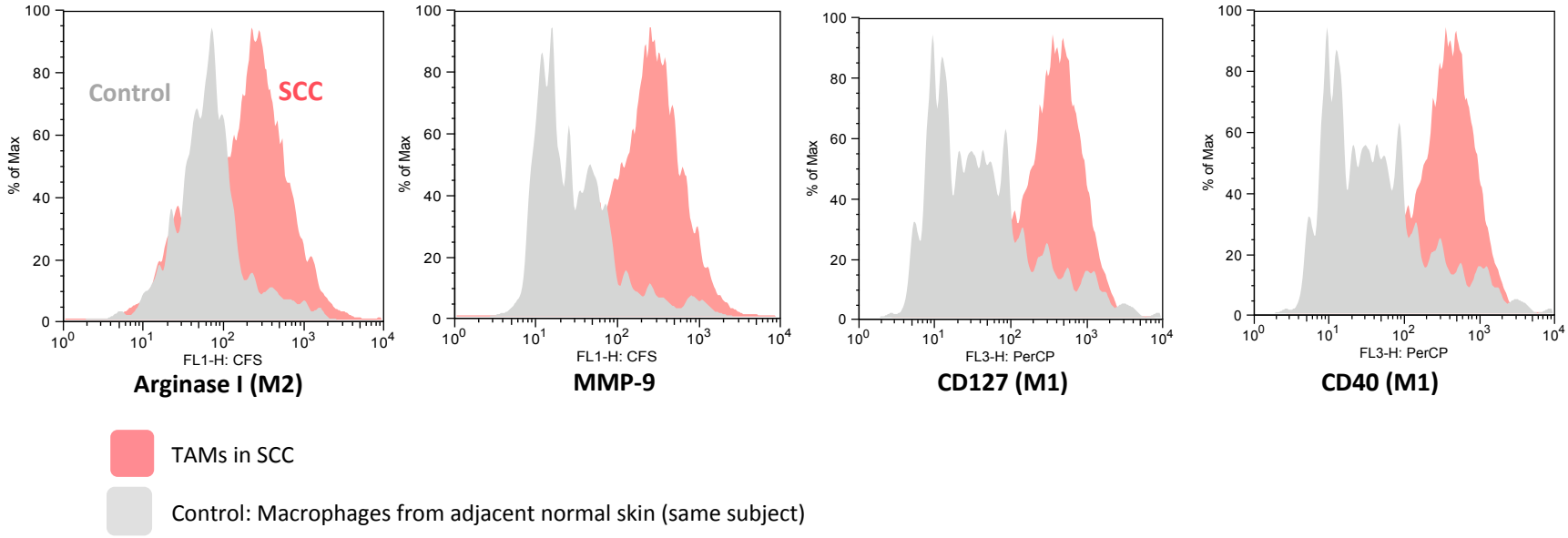

Figure 5 TAMs in cutaneous SCC are heterogeneously activated in comparison with peri-tumoral skin-resident macrophages

SCCs (n=3) and peri-turmoal normal skin (n=3) were used to compare CD68+CD45+ immunophenotype of TAMs as compared to skin-resident tissue macrophages. SCC from Mohs and the peri-tumoral normal skin from the same patient were used in each experiment. Tumors and peri-tumoral skin were digested using Liberase and prepared for flow cytometry. CD68+CD45+ cells were gated upon and histograms of arginase-I (M2), MMP-9, CD127 (M1), and CD40 (M1) were created for both SCC and peri-tumoral normal skin. The results shows that TAMs in SCC (red) have higher levels CD127, CD40, MMP9, and arginase I as compared to tissue-resident macrophages in peri-tumoral normal skin (grey).

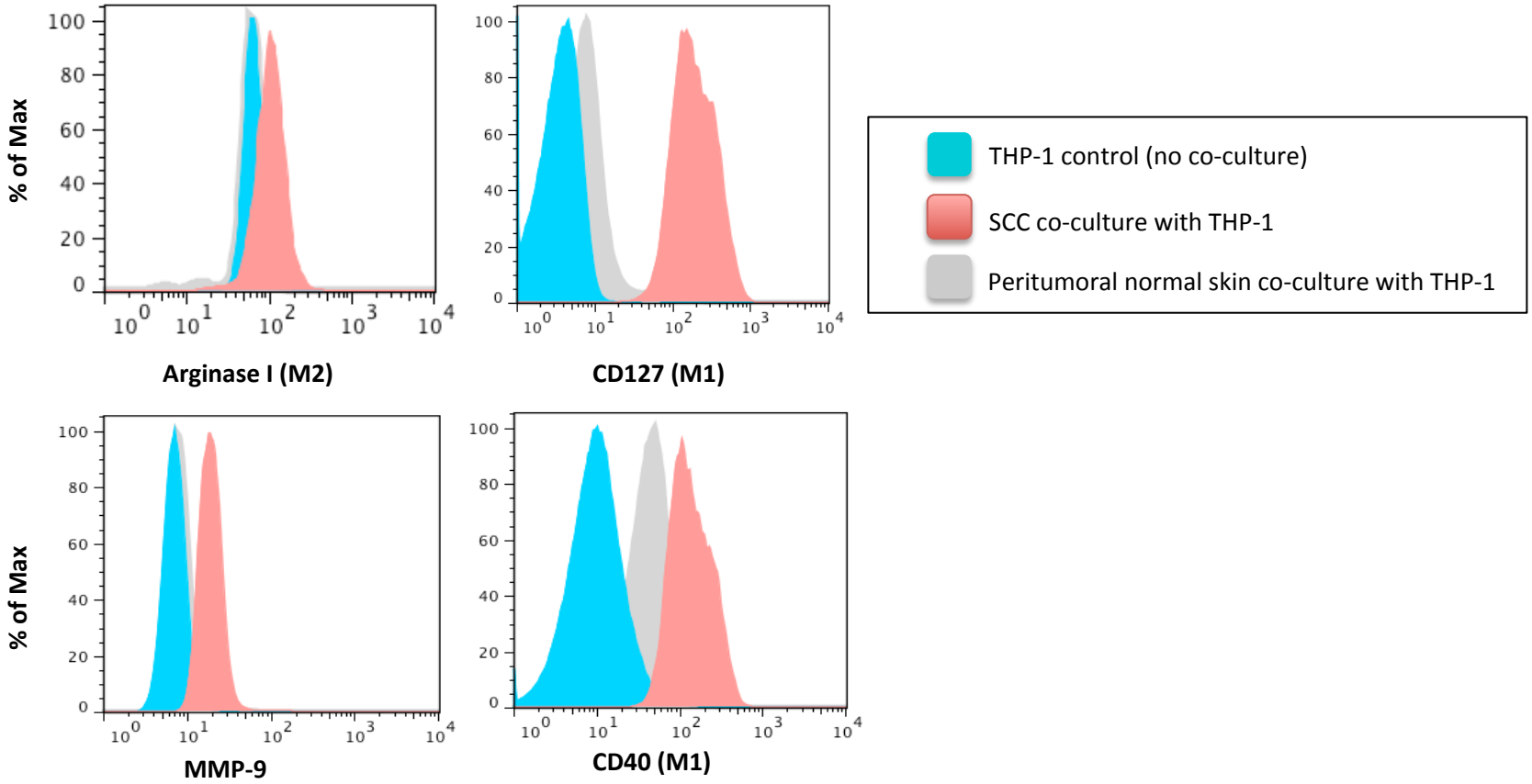

Figure 6 Co-Culture of Human SCC with Human monocytes (THP-1) leads to TAM programming characterized by M1 and M2 activation compared to peri-turmoal normal skin

SCC and peri-tumoral normal skin from the same patient were obtained from Mohs surgery. Tumor and peri-tumoral skin were manually minced and plated in RPMI complete in BD falcon culture insert with 1 µm PET membrane and transferred to six-well plate containing 1 million THP-1 cells in RPMI complete. After 72 hours, THP-1 cells were stained for FACS Immunophenotype (M1, M2, and MMP-9). CD68+ CD45+ cells were gated upon, and histograms representatives of arginase I, CD127, CD40 and MMP-9 are shown above. THP-1 cells co-cultured with SCC tumor cells have higher levels of M1 markers (CD40, CD127), M2 markers (arginase I), and MMP-9 compared to BCC and normal skin.

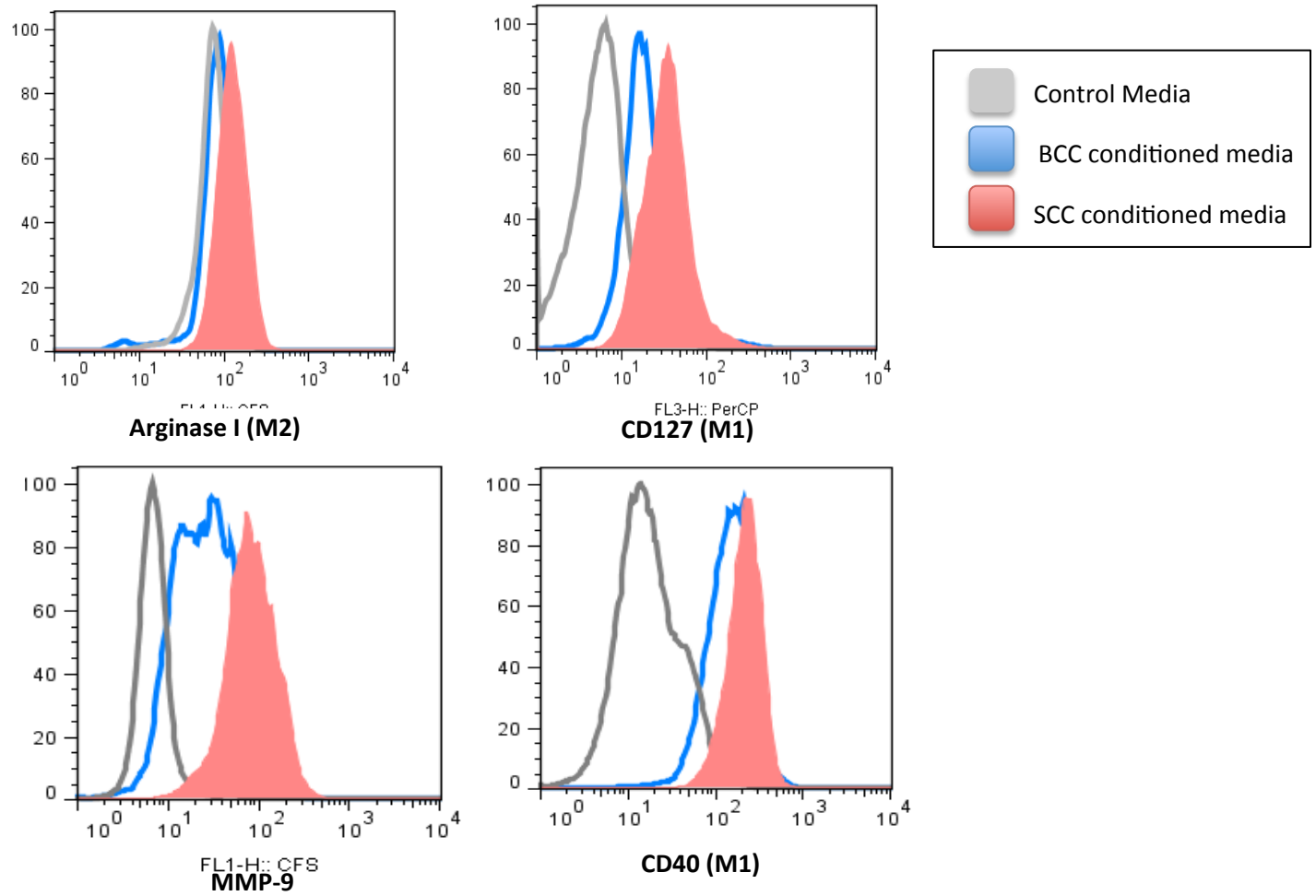

Figure 7 Polarization of THP-1s with SCC (red) and BCC (blue) conditioned media demonstrates distinct degrees of M1 and M2 activation

SCCs (n=3) and BCCs (n=3) tumors from MOHS were minced and placed in RPMI complete media in 37 ºC tissue culture incubator for 24 hours. The supernatants were then sterile-filtered. THP-1 cells were incubated in control RPMI, SCC-conditioned RPMI and BCC-conditioned RPMI. THP-1s were then analyzed using flow cytometry for CD40, CD127, arginase I, and MMP-9. THP-1 cells (red) incubated in presence of SCC-conditioned media have higher levels of M1 markers (CD40 and CD127), M2 marker (arginase I), and MMP-9 compared to THP-1 cells (blue) exposed to BCC-conditioned media. Control THP-1 cells are shown in grey and demonstrate baseline expression of these markers.

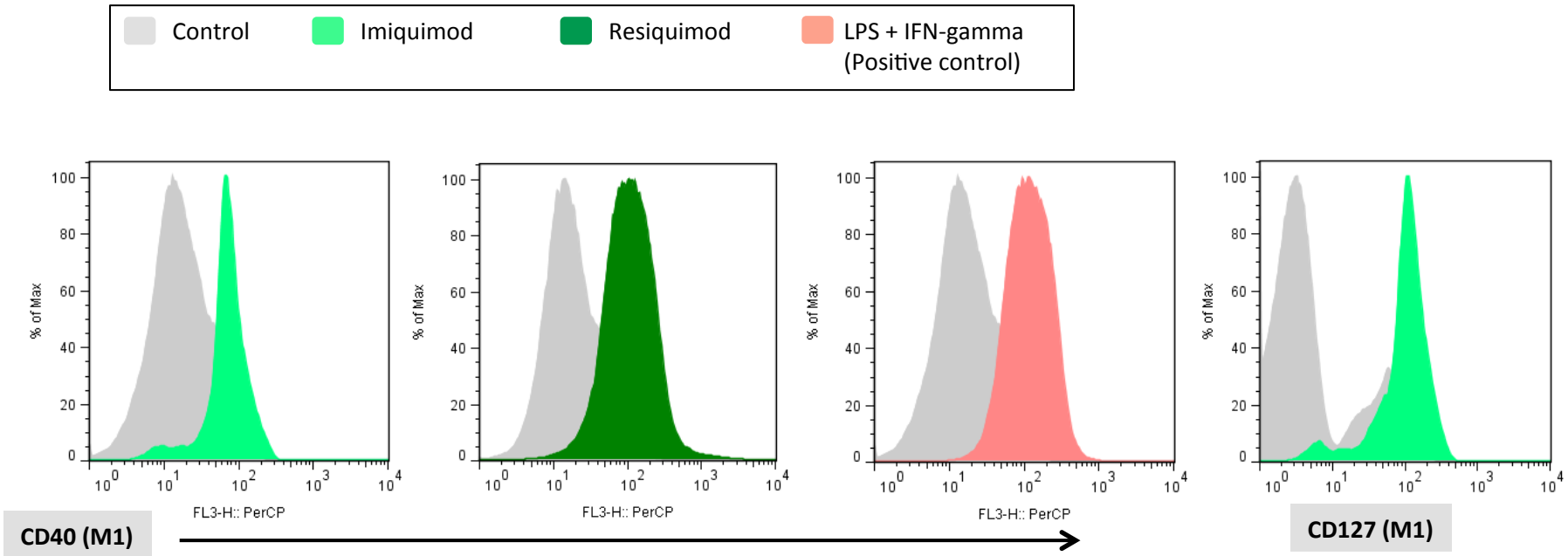

Figure 8 Imiquimod (50 ug/mL) and resiquimod (10 ug/mL) induce M1 activation of macrophages in vitro

THP-1 cells were plated and the following media were used for incubation: Control RPMI media (negative control), 50 µg/mL imiquimod in RPMI, 10 µg/mL resiquimod in RPMI, and 100 ng/mL lipopolysaccharide (LPS) and 20 ng/mL Interferon-gamma (positive control). After 48 hours, THP-1 cells were analyzed using flow cytometry for M1 markers (CD40 and CD127). CD68+CD45+ cells were gated upon and histograms of M1 markers were produced. Imiquimod and resiquimod induce marked M1 activation of THP-1 cells in vitro as shown by histogram shifts compared to negative control. The positive control of LPS and Interferon-gamma shows M1 activation as expected.

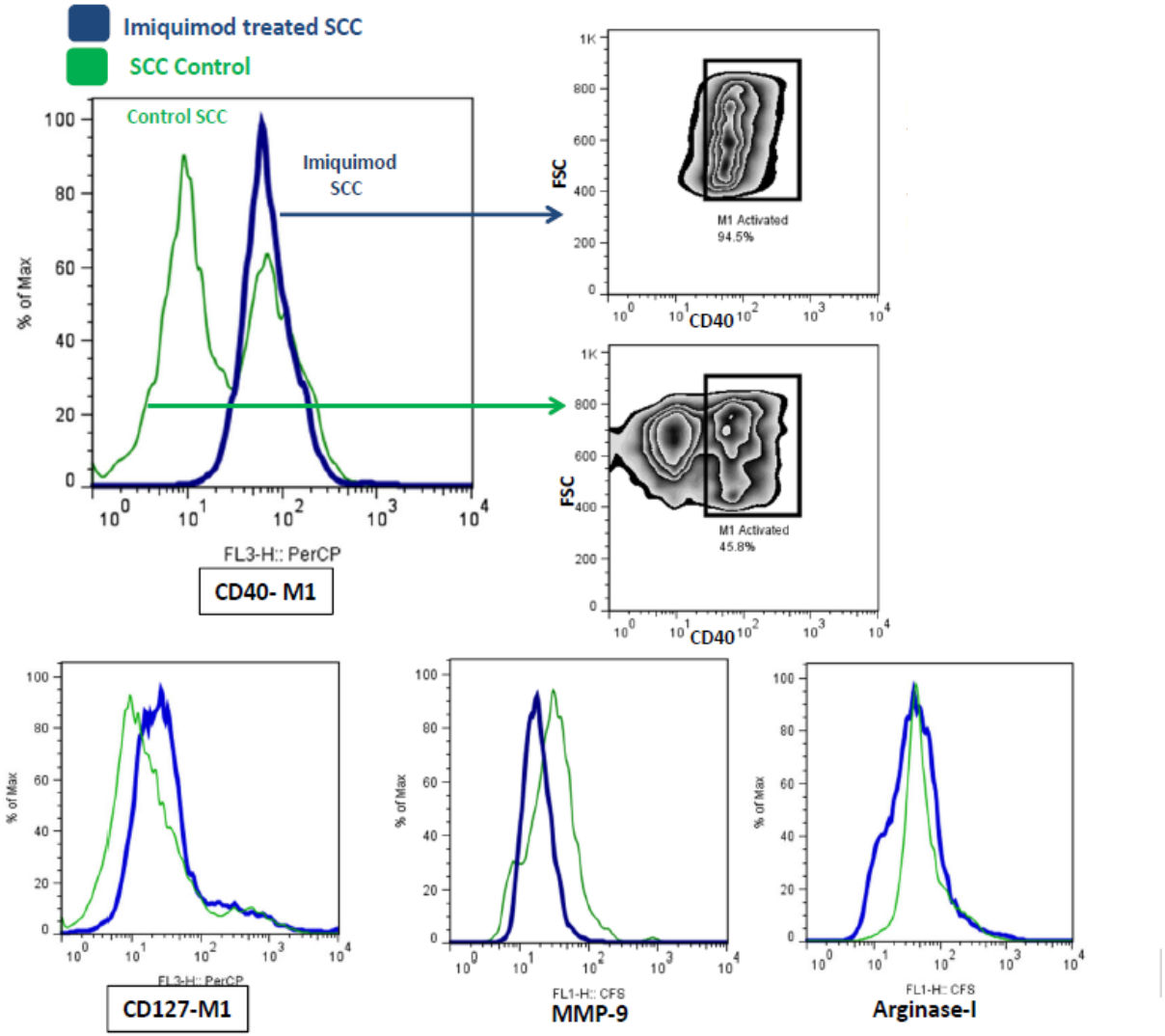

Figure 9 Imiquimod treatment of SCC in vivo induces M1 activation of tumor-associated macrophages

SCC from scalp of a patient treated with topical imiquimod (2.5 %) for 2 weeks was excised with Mohs and processed for flow cytometric immunophenotyping of TAMs. A similar SCC was used as control. CD68+CD45+ TAMs were gated upon and histograms of M1, M2, and MMP-9 were generated. 94.5 % of TAMs in imiquimod-treated SCC have M1 activation (CD40+) compared to 45.8 % of TAMs in control SCC. There is down-regulation of MMP-9 and no changes in arginase-I in TAMs from imiquimod-treated SCC compared to TAMs from control SCC.

Control media

BCC Supernatant

BCC supernatant + Imiquimod 50 µg/mL

SCC Supernatant

SCC supernatant + Imiquimod 50 µg/mL

M1 Uregulation by Imiquimod

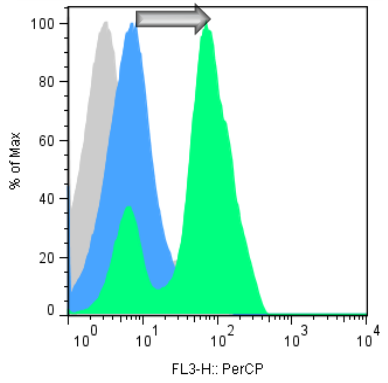

CD127

M2 Downregulation by Imiquimod

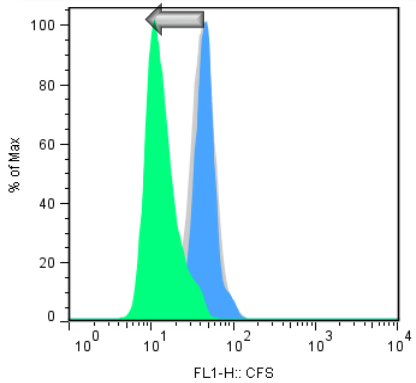

Arginase I

MMP-9 Downregulation by Imiquimod

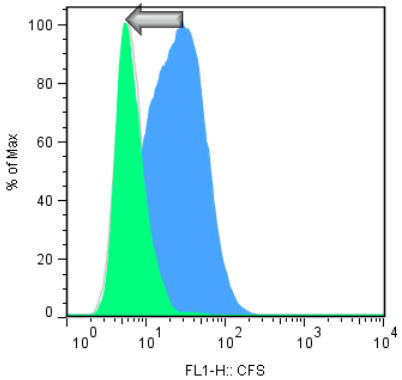

MMP-9

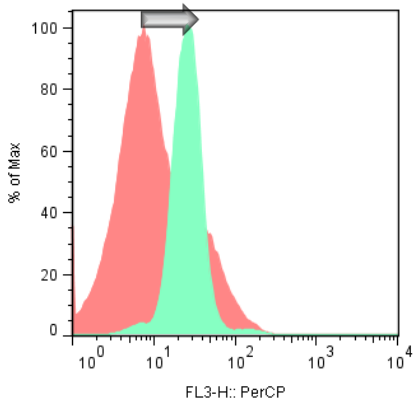

CD127

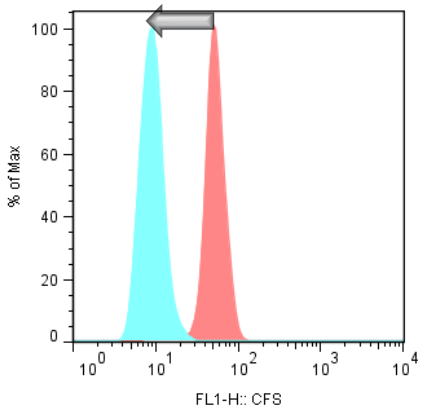

Arginase I

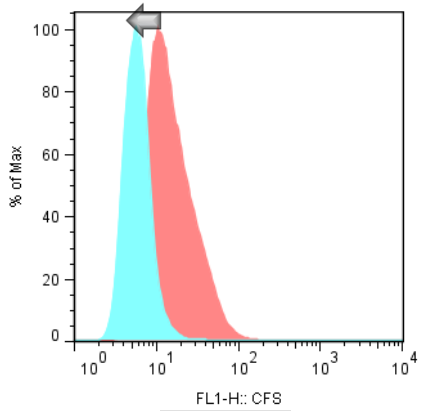

MMP-9

Figure 10 Imiquimod leads to immunomodulation of macrophages towards M1 and away from M2 in the presence of SCC- and BCC-conditioned media

Tumor-conditioned media from SCC and BCC was prepared through mechanical dissociation of tumors and incubation for 24 hours in RPMI complete. The media was then sterile-filtered with 0.45 μm filter. THP-1 cells were plated in BCC or SCC-conditioned medias in the presence of 50 μg/mL imiquimod or absence of imiquimod as the negative control. After 48 hours of incubation, THP-1 cells were prepared for flow cytometry of M1 and M2 markers, and MMP-9. In both THP-1 cells exposed to SCC-conditioned media and BCC-conditioned media, imiquimod leads to up-regulation of M1 markers (CD40 and CD127) and down-regulation of M2 marker (arginase I) and MMP-9. The arrows indicated the direction of immunomodulation in each graph. Therefore, imiquimod can acts as an immunomodulator of macrophages in presence of tumor-conditioned media.

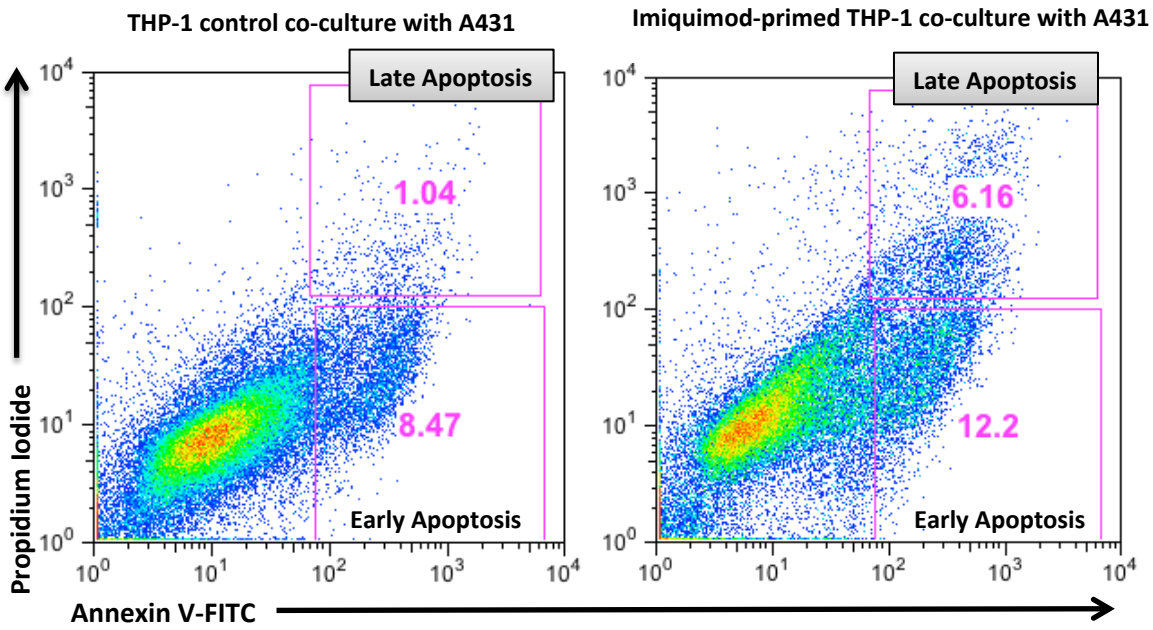
THP-1 control co-culture with A431
Imiquimod-primed THP-1 co-culture with A431
Late Apoptosis
Late Apoptosis
1.04
6.16
8.47
12.2
Early Apoptosis
Early Apoptosis
Propidium Iodide
Annexin V-FITC

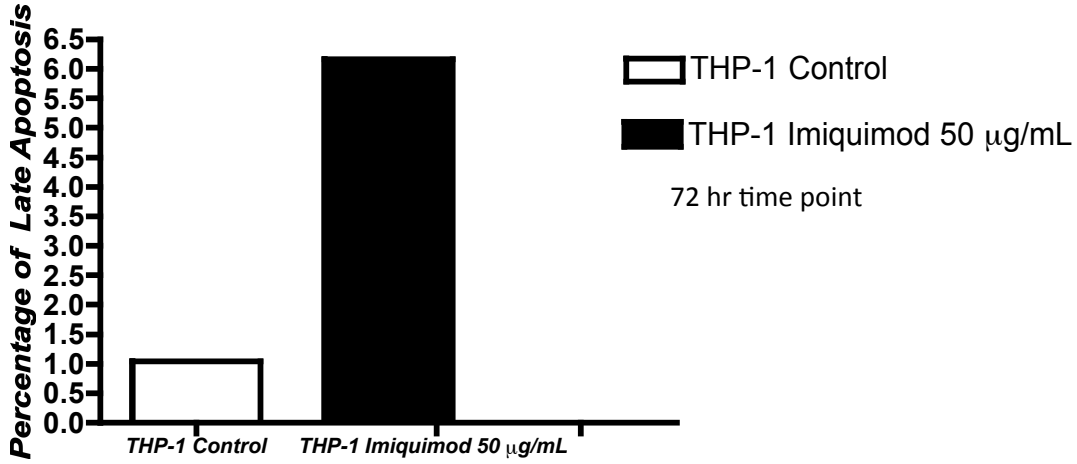
Percentage of Late Apoptosis
THP-1 Control
THP-1 Imiquimod 50 μg/mL
THP-1 Control
THP-1 Imiquimod 50 μg/mL
72 hr time point

Figure 11 Imiquimod-treated THP-1 cells induce enhanced apoptosis of human epidermoid carcinoma cells in a co-culture system

THP-1s were stimulated with 50 μg/mL imiquimod in RPMI complete and control RPMI complete for 48 hours. The supernatant was then aspirated carefully and the THP-1 cells were washed twice in cold PBS. A431 epidermoid carcinoma cells were plated in a six-well plate. THP-1 cells were placed in the upper Transwell insert. After 3 days of incubation, the level of apoptosis in the A431 epidermoid carcinoma cells was quantified using Annexin FITC and propidium iodide. The rate of early apoptosis (Annexin V+ Propidium Iodide -) is 8.47 % in control group and 12.2 % in the imiquimod group. The rate of late apoptosis (Annexin V + Propidium Iodide +) is 1.04 % in the control group and 6.01 % in the imiquimod group. The results suggest that imiquimod can enhance tumoricidal capacity of macrophage in a non-contact-dependent system as shown by increased levels of early and late apoptosis in human epidermoid carcinoma cells.

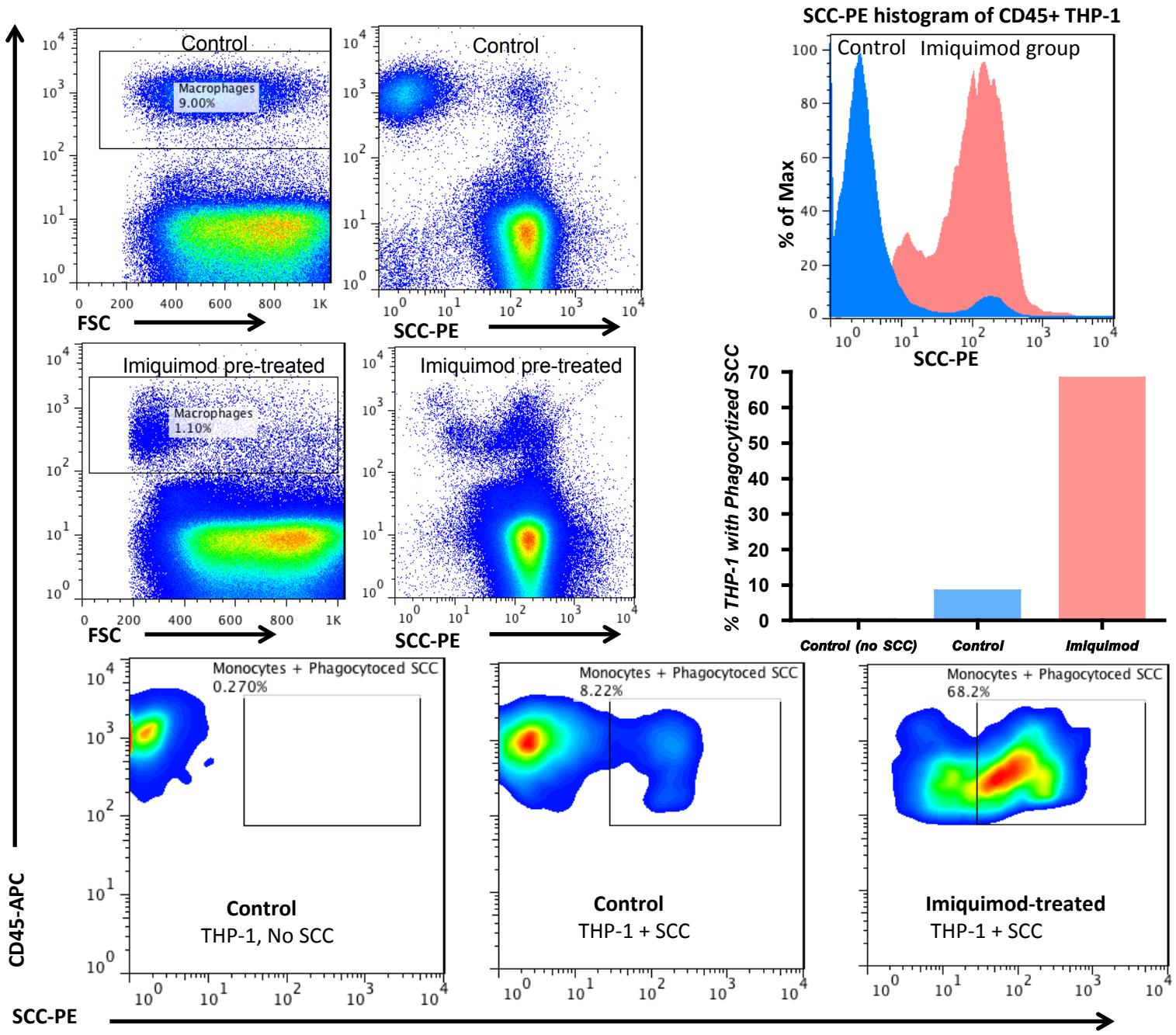
Control
Macrophages
9.00%
FSC
SCC-PE
Imiquimod pre-treated
Macrophages
1.10%
SCC-PE histogram of CD45+ THP-1
Control
Imiquimod group
% of Max
SCC-PE
% THP-1 with Phagocytized SCC
Control (no SCC)
Control
Imiquimod
Monocytes + Phagocytoced SCC
0.270%
Control
THP-1, No SCC
8.22%
THP-1 + SCC
68.2%
Imiquimod-treated
THP-1 + SCC
CD45-APC
SCC-PE

Figure 12 THP-1 cells primed with imiquimod phagocytose significantly more epidermoid carcinoma cells (A431) compared to control THP-1 cells

THP-1 cells were stimulated with 50 µg/mL imiquimod or control media for 48 hours. At the end of incubation, the media was aspirated and cells were wash twice in cold PBS. A431 epidermoid carcinoma cells were labeled with PE dye using PKH26 (Sigma Aldrich). Next, the control and imiquimod-primed THP-1 cells were mixed with A431 carcinoma cells in a ratio of 6:1 in conical tubes. The samples were then placed in a shaking incubator at 37 ºC for 1 hour at 200 rotations per minute. The samples were prepared for FACS using CD45 APC. CD45+ Cells were then gated upon to distinguish THP-1 cells from tumor cells. The rate of phagocytosis was determined by gating on CD45+ PE+ cells, which indicate marcophages that have phagocytosed PE-labeled tumor cells. The PE histogram of THP-1 cells in imiquimod group (red) shows significant shift compared to control group. Only 0.27 % of CD45+ THP-1 cells are positive for PE in the negative control without any tumor cells added. The rate of phagocytosis is 68.2 % in imiquimod-primed THP-1 cells as compared to 8.22 % in control THP-1 cells. These results suggest that imiquimod can enhanced the phagocytic capacity of macrophages for epidermoid carcinoma cells.

10 Known M1 genes are induced by imiquimod treatment of BCC

M1 Genes Induced by imiquimod
CD40
CCR7 (CD197)
CD86
CXCL9
CXCL10
STAT1
MX-1
CCL-2
CCL-3
CCL-4

- Panelli MC, Stashower ME, Slade HB, Smith K et al. Sequential gene profiling of basal cell carcinomas treated with imiquimod in a placebo-controlled study defines the requirements for tissue rejection. *Genome Biol* 2007;8(1)

Supplementary Figure 1- 10 known M1 genes are up-regulated by imiquimod treatment of BCC in a placebo-controlled study